Applied Geochemistry 137 (2022) 105179

Contents lists available at ScienceDirect

Applied Geochemistry

journal homepage: www.elsevier.com/locate/apgeochem

Central Hoggar groundwaters and the role of shear zones: $^{87}Sr/^{86}Sr$, $\delta^{18}O$, $\delta^{2}H$ and ^{14}C isotopes, geochemistry and water-rock interactions

M.E.H. Cherchali [a,*], J.P. Liégeois [b,**], M. Mesbah [d], N. Daas [a], K. Amrous [c], S.A. Ouarezki [a]

[a] Centre de Recherche Nucléaire d'Alger, Dpt Datation et Traçage Isotopique, 2, Bd F. Fanon, BP399, Alger-Gare, 16000, Alger, Algeria
[b] Geodynamics and Mineral Resources, Royal Museum for Central Africa, B-3080, Tervuren, Belgium
[c] Direction de l'Hydraulique de la Wilaya de Tamanrasset, Tamanrasset, Algeria
[d] Faculté des Sciences de la Terre, de la Géographie et de l'Aménagement du Territoire, USTHB-FSTGAT, Alger, Algeria

ARTICLE INFO

Editorial handling by Dr. I. Cartwright

Keywords:
Geochemistry
Environmental isotopes
Strontium isotopes
Central Hoggar
Algeria

ABSTRACT

In an environment of volcanic and plutonic rocks such as the Central Hoggar, the knowledge of groundwater flows and their residence time is of prime importance. This is especially the case in the arid zone of Central Sahara where the main town of southernmost Algeria, Tamanrasset, with its rapidly growing population (>200,000 inhabitants extreme South of Algeria), put an important pressure on the local aquifers. Central Hoggar belongs to the LATEA metacraton, which is a Precambrian basement largely fractured and invaded by Cenozoic mostly basaltic volcanic rocks. In addition to superficial alluvial reservoirs, these two contrasted lithologies and large and deep faults determine the geometry of the aquifers and the nature and composition of water. We show here that distinct aquifers exist along faults oriented from NW-SE to NE-SW with no lateral communications. Some waters are in equilibrium with the Cenozoic volcanic system and others with the Precambrian basement although the latter bear often a Cenozoic volcanic signature attributed to volcanic coating along faults at depth. Alluvial, volcanic and Precambrian aquifers display contrasted measured pCO_2 and specific conductivity (SC) values, stable ($\delta^{18}O$, $\delta^{2}H$), $^{87}Sr/^{86}Sr$, ^{3}H, $\delta^{13}C$ and ^{14}C isotopes. A major role is given to the Pan-African Adriane shear zone (ASZ), running just east of Tamanrasset, along which waters with high residence time ($0.2<A^{14}C<45$ pMC) are aligned in a 160–180 km long and 15 km wide corridor, including a natural soda spring (Tabahort). The latter have contrasted geochemical and isotopic signatures with respect to the other groundwaters originated from local evaporated precipitations. $^{87}Sr/^{86}Sr$ ratios vary from 0.70409 in volcanic aquifers to 0.72281 in Precambrian aquifers while C isotopes exhibit value from 0 to 117% pMC for ^{14}C activity and $\delta^{13}C$value from −12.5 to −2.12‰ vs VPDB. Trace elements are lower than the Maximum Admissible Concentration (MAC) except in the ASZ where Rb, Cs and U are found in higher concentrations elsewhere in Hoggar. This study enhances the peculiar status of the Central Hoggar groundwater aligned along the ASZ, close to the Tamanrasset City.

1. Introduction

In Central Hoggar desert region, southern Algeria, water quality and abundance are crucial parameters, especially in Tamanrasset, a rapidly growing town that has reached 250,000 inhabitants. A >750 km long water pipe-line from In-Salah has been recently built, engineered to deliver a volume of water of 50,000 m^3/day but actually delivering 25,000 m^3/day since 2011, due to the contribution of a lower number of production boreholes than initially planned. The In-Salah water is pumped from the "Continental Intercalaire" Cretaceous aquifer (Edmunds et al., 2003; Guendouz et al., 2003; Moulla et al., 2012; Cherchali et al., 2021) and is demineralized before use due to an elevated salinity (2–2.5 g/L). Despite this external supply, the local water table is essential for Tamanrasset as well as for the small remote localities that are not served by this external flow. It is therefore very important to know the geometry of the different deep aquifers, their possible interconnections and their reactions to the outlets and to confirm or deny whether the old concept of a single basement aquifer (Burgeap, 1975) can still be taken into consideration.

To this purpose, a geochemical and multi-isotopic approach was

* Corresponding author.
** Corresponding author.
E-mail addresses: mehcherchali@gmail.com (M.E.H. Cherchali), jean-paul.liegeois@africamuseum.be (J.P. Liégeois).

https://doi.org/10.1016/j.apgeochem.2021.105179
Received 15 August 2021; Received in revised form 13 December 2021; Accepted 16 December 2021
Available online 28 December 2021

carried out using major and trace elements, strontium isotopes ($^{87}Sr/^{86}Sr$), environmental isotopes ($\delta^{18}O$ and $\delta^{2}H$; water molecule), cosmogenic isotopes (^{3}H and ^{14}C) in groundwater in order to provide valuable information on the origin, mode of acquisition and transit time of water in aquifers.

Strontium is a group 2 lithophile trace element with an average concentration of 260 ppm in the Earth's crust. It is dispersed in some mineral lattices (e.g., feldspar or calcite) or is forming accessory minerals (e.g., strontianite, $SrCO_3$ or celestite, $SrSO_4$). In the hydrosphere, its concentration is mainly controlled by the solubility of these minerals. It is intensively used in groundwater studies (e.g., Clark and Fritz, 1997; Kendall and McDonnell, 1998; Négrel et al., 2004; Négrel and Casanova, 2005; Négrel, 2006) due to its ubiquity and to the existence of the radiogenic ^{87}Sr (resulting from the decay of ^{87}Rb, half-life of 50×10^{6} y) in addition to the stable 84, 86, 88 masses. Central Hoggar represents a favorable case for using Sr isotopes as it is composed of a Precambrian basement mainly made of granitoids and gneisses (Black et al., 1994; Liégeois, 2019 and references therein) and of Cenozoic volcanic rocks (mostly basalt and trachyte) of mantle origin particularly abundant and forming the highest mountains in Central Hoggar (Liégeois et al., 2005 and references therein). The Precambrian basement displays nowadays variable but always high $^{87}Sr/^{86}Sr$ (from 0.71 to 3.5 in whole-rock; Azzouni-Sekkal et al., 2003; Liégeois et al., 2003; Acef et al., 2003; Abdallah et al., 2007). On the opposite, the Cenozoic volcanic rocks cluster between 0.703 and 0.7045 (Liégeois et al., 2005 and references therein). These contrasted signatures imply that Sr isotopes constitute an excellent tracer for characterizing the Hoggar groundwaters relatively to these two major reservoirs.

Previous studies (Genet et Guyot, 1955; Cornet, 1957; Durozoy, 1959; (Idrotecneco-Sonarem, 1975); Saighi, 1999, 2001) have concerned respectively the Tin-Seririne basin (in the south Tassilian belts edge) and the Hoggar as a whole. These studies have approached characteristics of the aquifers by stable isotopes ($\delta^{18}O$, $\delta^{2}H$ and $\delta^{13}C$) but without deciphering the nature of the rocks with which water was in contact. In this study we aim at (i) updating the knowledge of the water resource, (ii) specifying the geochemical characteristics (age, geochemistry, strontium and stable isotopic ratios) of the different aquifer waters.

2. Geological and hydrogeological settings

2.1. Geological setting

Hoggar, South Algeria, is located in Central Sahara and constitutes the major part of the Tuareg shield, which represents a Cenozoic swell of 500,000 km^2 of Precambrian rocks associated with Cenozoic volcanism, consequence of the Africa-Europe collision (Liégeois et al., 2005; Rougier, 2013; Fig. 1A). The Tuareg shield is made of 25 Pan-African (late Neoproterozoic) terranes separated by shear zones (Black et al., 1994; Abdeslam et al., 2002; Liégeois, 2019). Central Hoggar is made of five terranes with similar characteristics, i.e. an Archaean-Paleoproterozoic basement overlain by Tonian to Ediacaran juvenile terranes and invaded by Ediacaran batholiths and plutons (Liégeois et al., 2003; Abdallah et al., 2007). They belong to the LATEA metacraton, LATEA being the acronym of the five constituting terranes, Laouni, Aouilène, Tefedest, Egéré-Aleksod, Azrou n'Fad (Liégeois et al., 2003; Bendaoud et al., 2008; Liégeois, 2019; Fig. 1A). To the west, LATEA is covered by the Silet juvenile terrane (Fig. 1A). During the main Pan-African orogenic stage (630-580 Ma), the LATEA Paleoproterozoic paleocontinent became a metacraton (Fig. 1; Liégeois et al., 2003, 2013) when it was dismembered by shear zones that induced displacement of several hundred kilometers and caused the emplacement of high-K calc-alkaline batholiths (Acef et al., 2003; Liégeois et al., 2003). During the Phanerozoic, these shear zones were frequently reactivated as shown by the variable thickness of Paleozoic and Mesozoic sedimentary deposits across the various Hoggar terranes (Beuf et al., 1971; Fabre, 2005). During the Cenozoic, the Europe-Africa collision reactivated again these shear zones, generating a swell and allowing the generation of the recent mostly basaltic volcanism (Liégeois et al., 2005; Azzouni-Sekkal et al., 2003; Rougier, 2013). The study area lies across the different LATEA terranes, including Silet (Fig. 1A), and so includes several major shear zones delineating these terranes. Among them, is the Adriane shear zone (ASZ), separating the Tefedest and Laouni terrane and running just east of Tamanrasset. Its name is derived from that of a volcanic tabular mountain, symbol of Tamanrasset city and elongated along the ASZ, showing the interplay between shear zones and volcanism. The ASZ being located close to Tamanrasset and being a major provider of water points, it is of paramount importance.

2.2. Hydrogeological setting

The Atakor plateau region (~2700 m) is the central highest zone of the Hoggar, most wadis (intermittent rivers) originating from this region (Fig. 2b). The relief is pronounced with steep slopes, generating a radial runoff with a well-marked drainage system over the poorly permeable Precambrian bedrock. Historically, Atakor floods have reached the Tin Tarabine wadi (300 km to the SE) as well as to the N and to the S (Igharghar wadis) and to the SW in the Tamanrasset wadi. The latter represents a relic of the ancient Tamanrasset River, which, more than 6500 years ago, flowed to the Cap Timiris Canyon in Mauritania (Skonieczny et al., 2015).

The mean annual air temperature/humidity is 22.8 °C/20.6% for Tamanrasset and 14.2 °C/37.3% for Assekrem (regional meteorological station of Tamanrasset; Fig. 3). The average annual rainfall and the total cumulative precipitation for the twenty-five last years are 59 mm and 1485 mm in Tamanrasset and 186 mm/4655 mm for the Assekrem with an evaporation rate from May to September of >4470 mm/year in Tamanrasset and about 3250 mm/year for Assekrem.

During this study, in agreement with the last twenty-five years, the main rainy season occurs from June to August while the lowest rainfall amounts are recorded from November to March and in May. Winter rains are less important than summer rains, indicating a more pronounced link with the Soudanese-Saharan monsoon and ITF (intertropical front) than with the Mediterranean rains and the polar front (PF). However large variations occur from year to year with several dry years followed by a wet season marked by heavy rainfalls being the double or more of the average annual value such as in 2005 when the total rainfall in Assekrem was 384.6 mm (vs annual average of 185 mm) causing flooding (Fig. S1).

In this study, we sampled three types of aquifers, all within the LATEA metacraton: (1) alluvial aquifers, (2) Cenozoic volcanic rock aquifers near Silet and Idelès (~135 km NE of Tamanrasset) and (3) fractured and altered Precambrian basement aquifers all over the study area (Fig. 1a, b, 2b).

Alluvial aquifers are located in the Quaternary wadi alluviums and in the underlying altered upper part of the Precambrian basement and are the primary water resource in Central Hoggar. Those investigated in this study (Fig. 2b) have an average thickness of c. 20 m, with an average depth for the static level of 7 m. The groundwater piezometric level may rise by 1–2 m after heavy rains and can decrease up to 4 m during long dry periods (e.g. 1972–1983). More recently, the combination of a long drought during the 2018–2020 period (no rain) associated to unrestrained pumping has led the piezometric level of the Tamanrasset alluvial aquifer to fall by 19 m.

Aquifers in volcanic basement result from an effective porosity of the volcanic rocks of c. 10%, with variable reactivity to rainfall events. The static level ranges from 1 to 5 m.

Aquifers in the Precambrian basement are linked to the fracture network, due to the very low porosity of granitoids and gneisses. As wadis often follow faults and shear zones, rain water are concentrated to these structures that can be locally very dense. Most of the Hoggar faults are subvertical down to a significant depth of several tenth of km

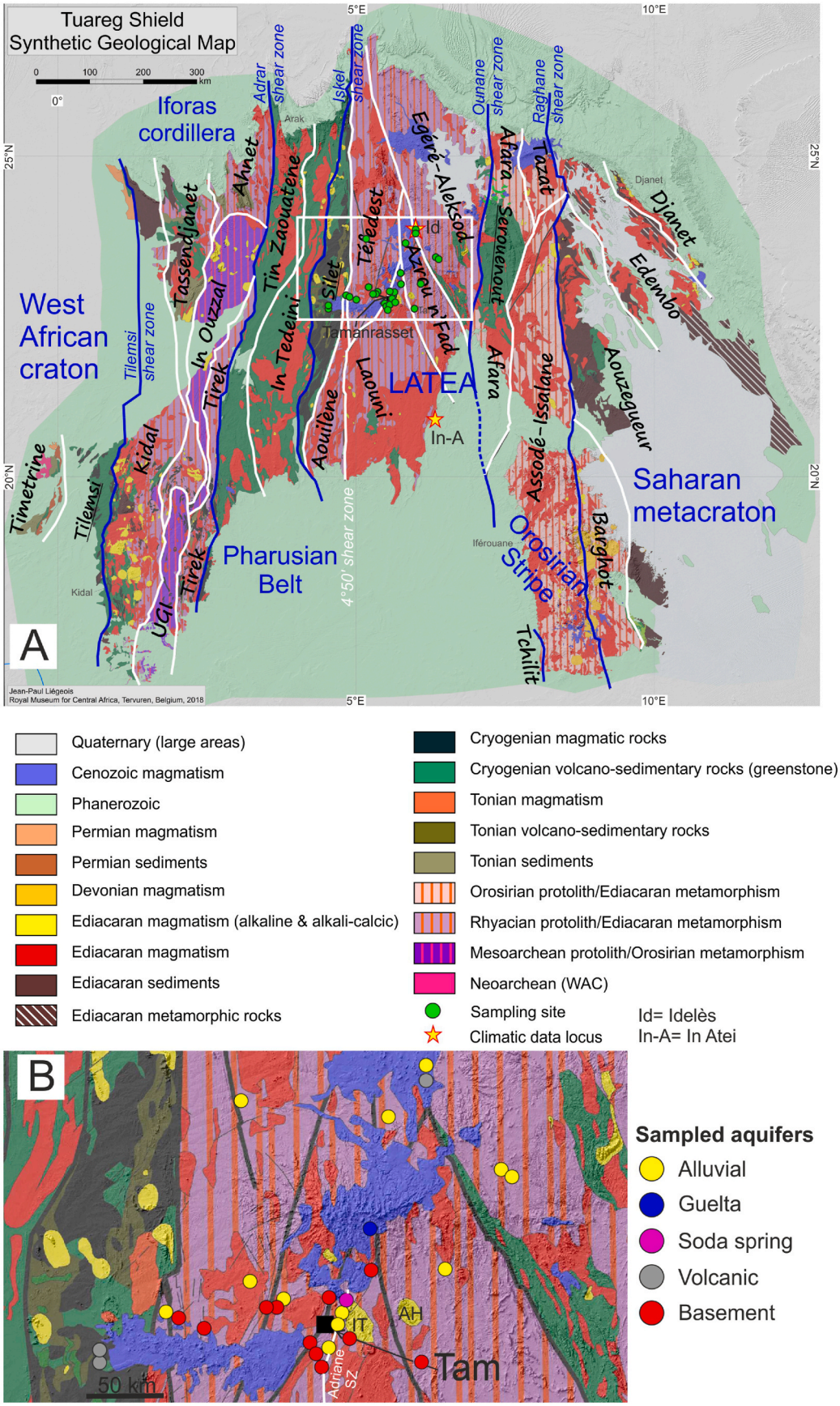

Fig. 1. (a) Latea metacraton (Central Hoggar) modified from Liégeois et al. (2003) reporting the water sampling points and the Adriane shear zone.

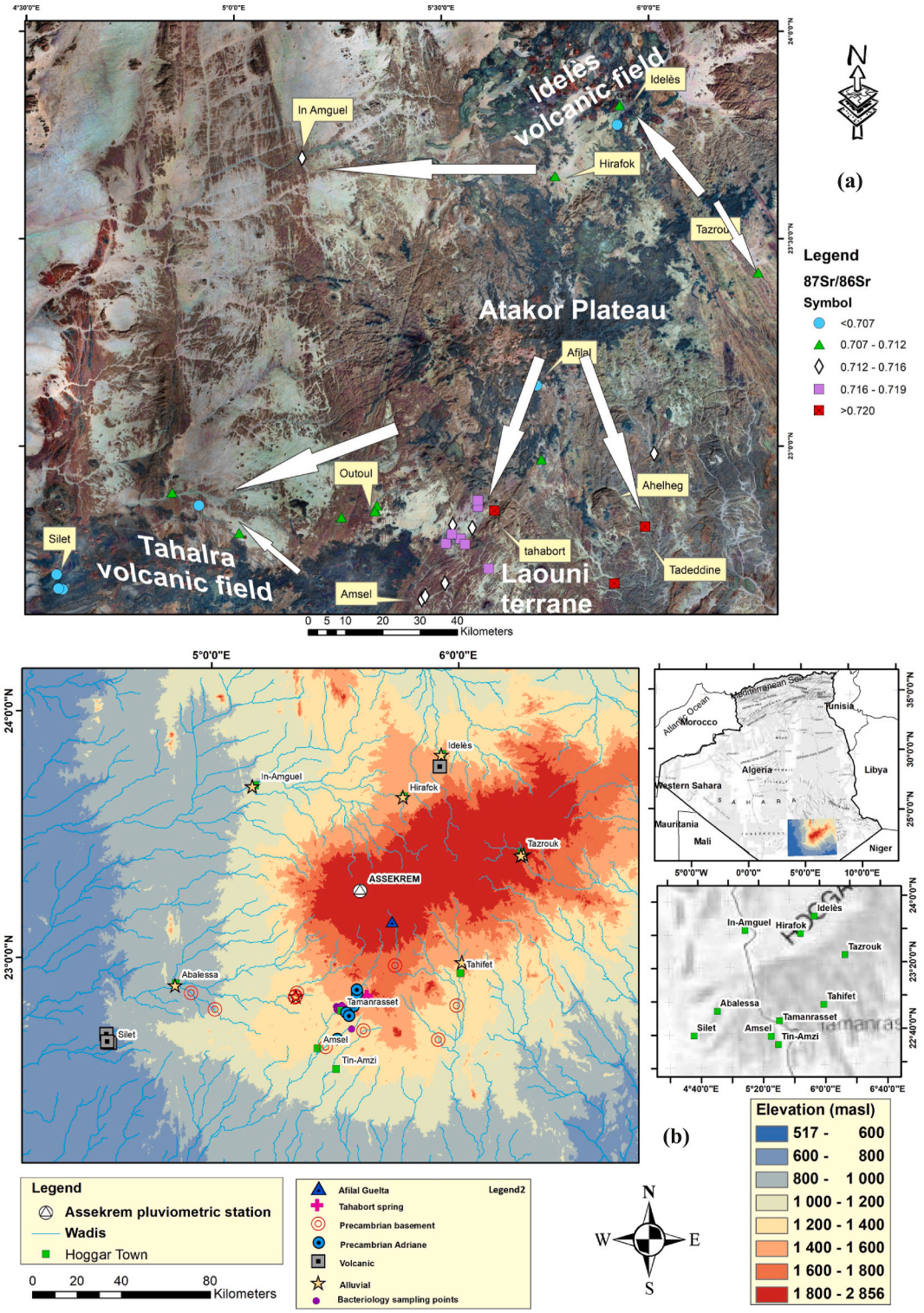

Fig. 2. (a) Map showing the inter-terrane Pan-African Adriane Shear Zone in the study area (the white arrows correspond to the flow direction) **(b)** Hoggar hydrologic map with water sampling localities and main towns.

(Bouzid et al., 2015), resulting in secondary porosities and permeabilities [A.N.R.H. Agence Nationale des ressources Hydriques, 1992]. Drillings performed within the basement generally do not exceed 100 m and are mostly dry.

The Water Resources Directorate of Tamanrasset has realized additional drillings since 1999, with an average depth of c. 35 m, with three having reached a depth of ~100 m. The latter are located within the Adriane shear zone (ASZ) area and correspond to Hog42, Hog45 and Hog70 samples (Fig. 2b). The ASZ extends to the North at least on ~135 km towards an old volcanic crater (Idelès El-Gueraret, sample Hog5 as

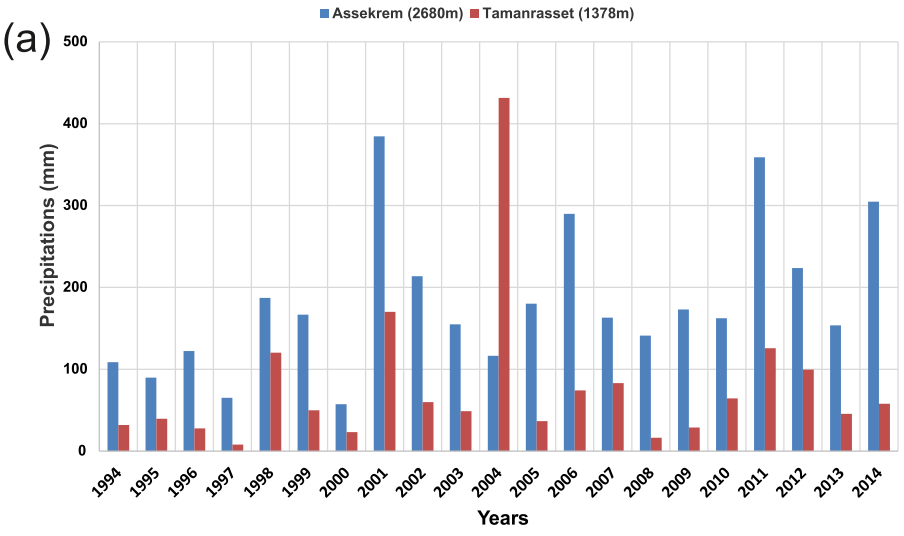

	J	F	M	A	M	J	J	A	S	O	N	D
Tam (1378m) Hum.%	22.6	22.3	18	15.3	15.1	17.3	16.5	22.2	22.8	24.8	24.7	25.7
ASK (2680m) Hum.%	33.2	33.9	31.5	32.8	33.2	37.1	32.7	40.4	42.9	45.1	43.3	41.2
Tam (1378m) T°	13.24	15.1	19.28	24.51	27.86	29.54	30.14	29.47	28.09	23.76	18.02	14.61
ASK (2680m) T°	7	7.82	11.21	15.56	18.17	19.32	20.22	19.5	18.24	14.57	10.48	8.13

Fig. 3. Climatic data and ombrothermic diagram for the central Hoggar.

well as to the south where two other boreholes have been studied (Hog80 at In-Zaouane and Hog78 at Amsel, Fig. 2b). The latter deliver fairly appreciable water inflows, with the largest one having a throughput mobilizing 30 l/s at the pump for a current operation rate of 4 l/s (F13).

3. Sampling and analytical methods

3.1. Sampling and analytical methods used in the field

More than 100 water points (dug wells, production wells, springs and guelta – small permanent ponds in desertic areas) were sampled during four field campaigns (Table S1). Major and trace elements, stable isotopes ($\delta^{18}O$ and $\delta^{2}H$) and strontium isotopes ($^{87}Sr/^{86}Sr$) have been acquired on 35 samples, $\delta^{13}C$ on 16 samples and ^{14}C on 18 samples. Some dug wells were sampled with a submersible pump Grundfos (4″), while production wells were sampled directly. Samples were taken after ensuring the equivalent evacuation of 3 times the casing and until the stability of the measured physico-chemical parameters was reached.

All the samples were collected in HDPE bottles with different volumes (1000, 500, 30 ml) according to the type of analysis to be carried out. Water temperature, pH, specific conductivity (SC), salinity (TDS) were determined in the field using a WTW 350i Multiline probe. The instrument calibration was made twice, the first one in the laboratory with standard pH solutions (4, 7 and 10) and a KCl known solution of (0.01 M/L) for SC (1413 µS/cm) at 25 °C and the second in the field. The dissolved oxygen (O_2) content was determined using a HACH-LDO^{TM}HQ10 luminescent probe calibrated in the open air. Water has been filtered in the field on a 0.45 µm filter. Measurements including alkalinity ($CaCO_3$) and nitrate (NO_3) were determined first by titration using H_2SO_4 0.16N or 1.6N and then using a HACH Dr890 field colorimeter; this allowed getting a rough estimate of the nitrate pollution in alluvial aquifers. The same analyses were repeated in the laboratory for checking.

3.2. Laboratory analytical methods

Chemical analyses for cations and anions were acquired on an ion

chromatograph Dionex120 rapid column. Analytical precision for cations and anions is 5–10%. Samples for cations analyses were acidified to pH = 3 (similar to ion chromatograph standards) with high purity HNO_3 (70.5%). Stable isotope $\delta^{18}O$ and $\delta^{2}H$ of the water molecule were determined in the Algerian Nuclear Research Centre (CRNA) with a continuous-flow isotope ratio mass spectrometer (CF-IRMS) Delta-V from Thermo Finnigan referring to well-established methods (Coplen et al., 1991, 2002; Kinga and Coplen, 2008). Measurements were made on 200 μL of water after equilibration (GasBench method) with CO_2 (24 h) for the $\delta^{18}O$ measurement and with Pt (Platin) rod (45′) for the $\delta^{2}H$. Values are in per mil (δ scale) against the international standard Vienna-Standard Mean Ocean Water (V-SMOW). After repeated (triplicate) measures of the standards, samples and internal standards, the analytical $\delta^{18}O$ and $\delta^{2}H$ accuracy is ±0.05‰ and ±1.0‰ respectively. $\delta^{13}C_{DIC}$ analysis were determined on CO_2 by means of the GasBench method attached to a continuous flow isotope ratio mass spectrometer (CF-IRMS) Delta-V after H_3PO_4 acidification (with pure 100% H_3PO_4, McCrea, 1950) from Total Dissolved Inorganic Carbon (TDIC) precipitated in the field. The values are given in per mil (δ scale) against the international standard V-PDB with an accuracy of ±0.1‰. ^{14}C activity has been determined in the radiocarbon laboratory of the CRNA by liquid scintillation measurements on benzene (C_6H_6) obtained from the TDIC precipitated in the field (from water volume of 60 or 120 L depending on the alkalinity) and ^{14}C contents are reported as percent of modern Carbon (pMC). Two sample's counting geometries are adopted, 2.25 and 4.5g, according to the amount of sample synthesized and mixed with respectively 0.5 and 1.5 ml of scintillation liquid. ^{14}C precision is for the geometry adopted with ^{40} K free-glass vials as background ≈0.61 ± 0.1 cpm and standard ≈32.13 ± 0.4 cpm. We consider that the activity of the sample obtained is real when it deviates from the background count rate from $A_s = B + 4\sigma$. For ^{3}H, the main performance parameters of the spectrometric system with 20-mL plastic vials and cocktail-to-sample ratio 12 + 8 ml and counting time of 600 min were as follows: background count rate 0.91 ± 0.15cpm and detection limit L_d of 2.0 TU (1 TU corresponds to 0.11919 Bq/L) according to (L'Annunziata M.F., 2003).

The Sr concentration as well as trace elements like (Rb, Cs, Ba, Mn, Fe, Cu, Zn, Al, Cd, Mo, Zr and U) and the Sr isotopic ratio, $^{87}Sr/^{86}Sr$, were measured in the RMCA (Royal Museum of Central Africa, Tervuren, Belgium) laboratory using an HR-ICP-MS (*Element2* of Thermo-Finnigan) for the elementary concentrations and using a multi collector Thermal Ionisation Mass Spectrometer (TIMS; VG-Sector54) for the Sr isotopic ratios. For isotopic measurements, an aliquot of 1–30 ml was evaporated (following Sr concentrations) before chemical separation on ion-exchange resins. Sr was separated using Eichrom B50 resin (Techno Inc.) and eluted with HNO_3. After separation, Sr was loaded on a tantalum filament. Measured $^{87}Sr/^{86}Sr$ isotopic ratios are corrected for mass fractionation using $^{86}Sr/^{88}Sr = 0.1194$ and normalized to the recommended value for the standard NBS987 = 0.710250. Each turret comprises 16 samples and 4 standards. During the course of the study, NBS987 gave a mean value of 0.710278 ± 0.000006 (20 values).

Physical-chemical parameters, major elements, stable isotopes ($\delta^{18}O$ and $\delta^{2}H$) and ^{3}H can be found in Table 1 while trace elements are reported in Table 2. $\delta^{13}C$, ^{14}C activity and corrected ^{14}C ages are available in Table 3. Table 4 gives Rb and Sr concentrations with Rb/Sr and $^{87}Sr/^{86}Sr$ strontium mean values used for the references representing the Hoggar groundwaters and Precambrian and Cenozoic volcanic basements. Table S1, S2 and S3 give respectively the water chemistry for all the field campaigns and $^{87}Sr/^{86}Sr$ for country rock and the basic information for all the sampling points.

3.3. Geochemical calculation

Calculations to assess dissolved speciation and saturation indices for the main mineral phases were undertaken using the Diagrammes program (*hydrochemistry multilanguage software*, *version* 6.*7*, Simler, 2020). The accuracy of cation and anion analyses are assessed through the charge balance error (CBE, ±5%). With the same program, calculated ^{14}C residence times in years before present (BP = 1950) has been made using the decay equation:

$$t_{age} = 8267 * \ln q \frac{a_0\,{}^{14}C_i}{a_t\,{}^{14}C_t} \quad (1)$$

where q is the proportion of DIC introduced via recharge and $^{14}C_i$ is the initial ^{14}C of DIC in the recharging water. Since the carbon isotopic content for both ^{14}C activity and $\delta^{13}C$ is affected by a dilution operated in the aquifer, the dilution of ^{14}C content is accounted for in the global equation by introducing the dilution factor q that is deduced from the chemical mass balance as follows (Clark and Fritz, 1997; Cartwright et al., 2020):

$$q = \frac{\delta^{13}C_{DIC} - \delta^{13}C_{carb}}{\delta^{13}C_{rech} - \delta^{13}C_{carb}} \quad (2)$$

The wide range observed in $\delta^{13}C$ values (−12.5‰ to −2.12‰; Fig. 7b) indicates different types of geochemical evolution of the carbonate system and different carbon sources. The most depleted $\delta^{13}C$ value (−12.5‰ vs PDB) is recorded in the Tahalra volcanic province (Silet district basalt) (Fig. 7b), west of the ASZ, suggesting that the soil-CO_2 contribution is the principal source of carbonate species in shallow volcanic groundwaters and in alluvial aquifers. Alluvial aquifer water samples display depleted $\delta^{13}C$ values between −12.5 and −8.35‰ vs V-PDB, interpreted as a mixing with C coming from the soil-CO_2 gas (−21‰ vs. VPDB; Guendouz, 1985). Following these calculations, models based on chemical parameters involved in the media (chemical mass balance-CMB, ALK-model) or on $\delta^{13}C$ isotope (Pearson and Hanshaw, 1970; Fontes and Garnier 1979) or on both, have been developed to correct the initial ^{14}C activity of the TDIC (*Total Dissolved Inorganic Carbon*) (Reardon and Fritz, 1978; Fritz and Fontes, 1980; Clark and Fritz, 1997; Cook and Herczeg, 2001; Cartwright et al., 2020).

4. Results

4.1. Chemical results

Ground and surface waters have been sampled in Central Hoggar especially along the ASZ (Fig. 1b; 2a). The Hoggar groundwater SC is between 152 and 1806 μS/cm (Table 1) with the highest values coming from the ASZ. The different hydrochemical water types are shown in Fig. 4. Three types have been recognized: (1) Sodium-bicarbonate, (2) Calcium–Magnesium-bicarbonate and (3) Magnesium-bicarbonate. For cations, the relative abundance is Na > Ca > Mg or Ca > Mg > Na and for the anions HCO_3>Cl > SO_4. In the vicinity of Tamanrasset, an anthropic pollution by nitrates (NO_3^-) is noted, which exceeds five times or more the MAC (45 mg/l) and this for more than 17 production wells. In two of them, a values 700 mg/l (16 times the MAC; Table S1).

4.2. Isotopic results

4.2.1. Stable isotopes

Groundwaters were analyzed for stable isotopes during three main periods (2002, 2004, and 2007, Table S2). For alluvial, volcanic and Precambrian waters, $\delta^{18}O$ and $\delta^{2}H$ values are respectively −5 to +5‰, and −25.6 to 6‰, −4.9 to-2.82‰ and −30.9 to −21.3‰, −5.8 to −1.7 and −36.5 to −9.78‰ vs VSMOW. Only one sampling point, Tahabort spring, exhibit much depleted values with an average value ~ -9.6‰ in $\delta^{18}O$ and ~-65.6‰ in $\delta^{2}H$ vs VSMOW. All the samples (Fig. 7a) lie on or

Table 1
Hydrochemical and isotopes results for both alluvial and basement aquifers.

ID	Type	pH	T°C	pCO_2	SC	TDS	Alk	Ca	Mg	Na	K	Cl	SO_4	HCO_3	NO_3	F	SiO_2	Sr	Li	$\delta^{18}O$	$\delta^{2}H$	*d*	^{3}H
			°C	Atm	µS/cm	mg/L														‰ vs VSMOW			T.U
Alluvial aquifers																							
Hog2t	W	7.11	18.4	0.0107	319	157	126.6	36	8.9	17.6	2.67	6.64	22.1	154.4	2.69	0.42	21	0.341	0.21	nd	nd	nd	7.7
Hog3	W	7.22	18.7	0.0099	347	169	151	42.2	9.5	19.9	2.5	7.31	25.1	184.1	3.77	0.46	18.7	0.381	<DL	nd	nd	nd	7.7
Hog4	W	6.68	21.9	0.0415	386	192	174	36.2	12.4	27.9	2.95	7.39	17.5	212.2	nd	0.56	23.4	0.355	<DL	−4	−21.4	10.4	5.6
Hog7	W	6.75	23.1	0.0306	591	291	151	56.6	15	57.3	4.12	16.3	32.8	184.1	5.82	1.14	27.7	0.515	0.18	nd	nd	nd	nd
Hog9	W	7.25	19.5	0.0155	528	263	253.4	52.6	14.3	50.3	2.55	6.08	19	308.9	7.32	0.85	29.2	0.536	<DL	−4.1	−23.4	9.4	21.7
Hog13b	W	7.53	25.9	0.0111	879	437	325	22.9	25.4	163	5.13	59.6	52.9	396.3	2.81	0.45	29.8	0.591	<DL	−4.2	−21.9	11.7	nd
Hog51	B	7.21	25.3	0.0088	327	167	76	31.7	15.7	20.8	2.56	13.8	46.2	146.4	13.5	1.32	26.4	0.276	<DL	−2.28	−11.0	7.2	nd
Hog69	B	7.18	18.6	0.0092	732	364	128	30.1	8.1	20.8	2.74	41.7	88.1	156	14.1	0.63	26.4	0.1329	<DL	−2.9	−16	7.2	8.6
Volcanic basement aquifer																							
Hog5	W	6.79	30.5	0.1374	1806	906	910	36.7	164.5	60.7	44.2	7.84	20.11	946.9	29.8	0.5	74.8	0.710	<DL	−4.1	−31	1.8	<DL
Hog30	W	7.52	27.4	0.0092	571	283	259.8	87	21.4	57.9	4.51	57.8	32.2	316.7	36.9	0.75	45.3	0.534	<DL	−4.4	−27.1	8.1	15.4
Hog30b	W	7.57	29.2	0.0058	503	249	172.7	26.3	19.8	55.9	5.56	37.8	19.8	210.6	5.95	0.6	40.4	0.437	<DL	−4.9	−27.6	11.6	nd
Hog33	W	7.78	28	0.0043	870	432	222.7	91.7	15.1	39.9	2.2	29.1	24.8	271.5	3.61	0.87	45.1	0.890	0.18	−4.4	−27.1	8.1	nd
Hog35t	W	6.73	25.8	0.0597	771	380	281.5	84.7	35.9	66.9	2.14	22.7	61.6	343.2	7.8	0.64	34.2	0.717	<DL	nd	nd	nd	nd
Spring Tahabort																							
Hog16*	S	5.82	21.4	0.6194	703	349	364.7	60.5	6.3	108	13.1	9.23	12.6	444.6	3	2.53	54.1	0.297	0.45	−9.7	−65.6	12	2.1
Precambrian basement, Adriane shear zone																							
Hog42*	B	5.95	27	0.6176	1415	703	470.9	126	34	246	12.2	27	32.6	574.1	nd	0.81	56.7	0.708	0.61	−4.8	−31.4	6.9	2.3
Hog45*	B	6.8	26.5	0.0566	1168	586	302	100	44.2	145	10.6	20.1	42	368.2	nd	1.07	49.9	0.807	0.39	−3.8	−32.1	−1.7	<DL
Hog70*	B	5.82	26.6	1.0576	1050	524	738.1	103	47.1	106	9.45	23.5	62.53	738.1	0.85	0.97	45.9	0.276	0.63	−4.5	−30.8	5.2	<DL
Hog76*	B	6.57	23.5	0.1006	908	450	325.3	87.2	19.4	30.8	3.91	56	43	396.6	46.1	0.99	36.6	0.933	<DL	−3.8	−22.6	7.8	<DL
Hog77*	W	6.4	24.7	0.1112	1366	680	257.2	158	47.5	86.2	2.38	129	269	313.6	30.5	1.69	35.7	0.1105	0.18	−2.5	−9.23	10.8	6.9
Hog78*	B	6.14	25.7	0.4111	1089	538	478.6	79.9	39	60.5	7.08	6.93	11	583.5	nd	1.27	73.2	0.610	0.19	−4.3	−24.9	9.5	3.5
Hog80*	B	6.16	23	0.2839	1403	699	378.8	105	32.8	236	3.36	25.8	152	461.8	13.2	0.6	40.6	0.973	0.18	−5.9	−36.2	11	<DL
Precambrian basement aquifer (general)																							
Hog82	B	7.52	24.2	0.0042	396	201	143.4	65.9	10.98	34.33	2.04	55.29	31.81	183	64.61	0.76	34.3	0.703	<DL	−4.4	−23.4	11.8	<DL
Hog84	B	7.22	24.6	0.0071	312	155	98.5	31.57	7.48	22.02	3.61	10.26	19.43	120.1	18.71	0.62	24	0.296	<DL	−2.9	−31.8	−8.6	7.4
Hog86	B	7.4	27.5	0.0076	625	313	222.6	43.3	18	56.5	2.3	65.7	26.7	196.6	10.64	1.2	37.3	0.512	<DL	−2.1	−14.6	2.2	6.3
Hog91	B	7.5	34	0.011	1076	540	303	68.64	20.09	172.1	5.44	176.1	173	369.1	12.78	0.61	20.3	0.732	<DL	nd	nd	nd	2.3
Hog92	B	6.93	25.5	0.0222	460	227	158.6	43.7	14.1	23.3	2.4	12.63	33.7	193.4	15.57	1.46	25.3	0.377	<DL	−2.8	−16.1	6.3	5.3
Hog96	B	7.6	20.2	0.0043	337	168	152.2	29.52	7.23	49.27	1.86	6.58	23.78	185.6	7.39	2.16	23.1	0.276	<DL	−3.7	−21.5	8.1	8.7
Hog97	B	7.38	20.8	0.0059	309	154	124.1	28.11	5.27	32.91	3.2	6.35	13.47	151.3	8.99	0.38	22.2	0.333	<DL	−1.7	−12.5	1.1	6.2
Hog98	B	7.44	25.1	0.0046	801	396	110.1	81	22.7	25.5	3.8	60.52	47.9	134.2	163	0.55	20.1	1.38	<DL	−2.9	−14.5	8.7	4.8
Hog99	B	7.27	20.4	0.0076	299	152	128	30.1	8.3	16.7	3.3	4.93	16.81	156	6.4	0.63	19.3	0.362	<DL	−2.4	−13.1	6.1	4.7
Hog100	B	7.56	20	0.007	508	256	235.5	60.47	13.83	35.6	1.46	4.67	15.1	287.1	2.69	0.93	25.7	0.432	<DL	−3.6	−17.6	11.2	8
Hog101	B	7.29	23.8	0.0065	922	420	112.6	38.7	17.8	43.8	2.3	42.54	77.07	137.3	24.6	2.51	31.5	0.58	0.23	nd	nd	nd	nd
Hog102	B	7.12	22.5	0.0114	489	242	131.8	24.2	16.2	26.6	2.53	12.09	38.05	160.7	8.29	0.61	28	0.506	<DL	−4	−21.6	10.4	3
Afilal Guelta																							
Hog103	G	8.12	18.7	0.0022	655	329	276.4	13.6	32.3	43	9.2	9.45	11.76	337	11.6	0.38	23.2	0.739	<DL	−3.9	−20.9	10.3	5.3

Table 2
Trace elements concentration in the different aquifers around the Hoggar.

ID	Al(200)	Ba(100)	Fe(200)	Mn(50)	Zn(5000)	Mo(100)	Cd(3)	Pb(10)	Rb	Cs	U(15)
µg/L											
Alluvial aquifers											
Hog2t	23,4	73	34,22	2,74	6,7	1,64	0,04	1,52	0,23	0,00	0,52
Hog3	21,1	83	27,69	1,46	10,3	1,71	0,03	1,91	0,17	0,00	1,17
Hog4	27,5	74	37,18	2,69	11,2	1,72	0,05	1,51	0,26	0,00	0,41
Hog7	26,4	88	25,80	0,72	17,4	3,90	0,04	1,01	0,53	0,00	5,46
Hog9	32,6	66	32,50	7,69	338,3	3,75	0,09	3,12	1,40	0,02	6,46
Hog13b	**287,3**	**144**	61,47	36,64	59,7	7,03	0,04	0,64	43,78	0,01	**16,30**
Hog69	22,8	**111**	54,46	1,64	49,2	10,98	0,06	0,50	0,16	0,00	8,16
Spring Tahabort											
Hog16	23,2	**155**	92,55	30,17	23,9	6,76	0,16	4,09	0,71	1,72	5,36
Precambrian basement, Adriane shear zone											
Hog42	23,9	59	91,77	71	10,0	11,70	0,06	2,25	37,83	1,15	0,92
Hog45	17,0	**105**	**866,50**	**122**	17,2	13,13	0,06	0,76	20,77	1,07	1,20
Hog70	2,0	**111**	0,11	**121**	838,1	4,79	0,06	0,33	37,03	2,07	1,37
Hog76	24,0	41	125,24	**102**	171,2	4,93	0,07	2,42	2,11	0,08	11,51
Hog77	34,3	**230**	**587,31**	22	14,7	6,85	0,05	0,80	1,05	0,09	**42,6**
Hog78	11,3	**268**	**74895,25**	**761**	412,7	1,65	0,03	0,71	3,75	0,13	1,17
Hog80	16,5	91	74,31	8,78	85,1	2,64	0,05	0,69	0,51	0,02	**26,11**
Volcanic basement aquifer (Idelès, Silet) and alluvial Abalessa											
Hog5	0,3	6	0,17	0,07	0,5	13,24	0,03	0,49	32,33	0,03	0,02
Hog30	27,8	55	65,94	1,45	9,6	18,99	0,08	0,78	0,48	0,00	0,87
Hog30b	46,0	22	47,03	1,80	11,0	15,63	0,08	1,34	5,16	0,01	0,25
Hog33	40,8	95	46,84	1,65	8,0	17,06	0,08	1,70	0,73	0,01	1,38
Hog35ter	47,2	**212**	63,57	2,50	10,1	2,95	0,03	6,40	0,32	0,00	9,63
Precambrian basement aquifer (general)											
Hog84	30,2	77	49,45	4,34	115,9	5,98	0,06	2,65	0,33	0,00	0,65
Hog86	15,0	81	46,40	2,21	37,7	86,38	0,31	0,70	0,09	0,00	2,53
Hog91	28,1	**125**	89,65	17,11	749,4	4,02	0,08	2,93	1,27	0,03	11,19
Hog92	77,5	80	90,14	2,63	34,2	6,20	0,07	1,12	0,47	0,01	2,83
Hog96	32,9	72	111,39	22,42	131,6	6,61	0,04	1,02	0,56	0,00	2,72
Hog97	22,1	58	24,98	0,87	148,2	5,75	0,04	1,11	0,57	0,00	0,18
Hog98	16,7	**111**	103,29	21,95	1541,7	4,33	0,05	0,78	0,69	0,01	2,93
Hog99	36,1	41	53,11	2,05	107,6	5,16	0,10	1,11	0,20	0,01	0,91
Hog100	41,8	**107**	138,94	11,71	311,2	11,14	0,06	1,40	0,53	0,00	3,55
Hog101	82,4	**175**	94,46	2,18	12,8	5,91	0,04	1,01	0,18	0,01	**29,16**
Hog102	30,5	81	41,03	1,60	6,6	6,02	0,04	0,69	0,09	0,00	1,26
Afilal Guelta											
Hog103	57,7	**105**	97,71	19,62	5,1	5,49	0,06	0,36	1,43	0,00	2,56

Table 3
^{14}C activity, $\delta^{13}C_{meas}$, $\delta^{13}C_{eq}$, raw and corrected ^{14}C ages.

ID	Localization	Type	X-Long	Y-Lat	$\delta^{13}C$	^{3}H	$A^{14}C$	Raw Age	Pearson	Clark&Fritz	Ferronsky	Average
					‰PDB	T.U	pmC	ka				
Alluvial aquifer												
Hog51	Ezerze	B	5.5667	22.7097	−11.51	nd	117.4	modern	modern	modern	modern	modern
Hog69	Outoul	B	5.34194	22.8453	−7.84	8.6	71.4	260	modern	modern	modern	modern
Volcanic basement aquifer												
Hog5	Ideles	W	5.9247	23.7742	−2.29	<DL	5.1	24,630	6.300	6.300	7.800	6.790
Hog30	Silet	W	4.5725	22.6903	−12.5	15.4	nd	nd	nd	nd	nd	nd
Hog30b	Silet	W	4.5872	22.6547	nd	nd	nd	nd	nd	nd	nd	nd
Hog35t	Abalessa	W	4.8599	22.8891	−8.36	nd	nd	nd	nd	nd	nd	nd
Spring Tahabort												
Hog16	Tahabort	S	5.628333	22.844167	−2.63	2.1	0.2	>30.000	>30.000	>30.000	>30.000	>30.000
Precambrian basement. Adriane shear zone												
Hog42	Adriane	B	5.5753	22.8028	−3.47	<DL	1.6	>30.000	19.300	19.260	20.800	19.780
Hog45	Pic Iharen	B	5.5892	22.8536	−4.08	2.3	3.7	27.260	13.710	13.690	15.200	14.200
Hog70	Pic Iharen	B	5.5892	22.8675	−3.92	<DL	3.2	28.460	14.580	14.530	16.000	15.000
Hog76	In Kouf	B	5.5468	22.7761	−4.59	<DL	13.2	16.740	4170	4150	5.700	4.700
Hog77	Amsel	W	5.5094	22.6694	−5.95	6.9	31	9.680	modern	modern	modern	modern
Hog78	Amsel	B	5.54583	22.77611	−4.27	3.5	3.9	26.800	13.650	13.600	15.100	14.100
Hog80	In Zaouane	W	5.5575	22.7631	−2.12	<DL	12.2	17.400	modern	modern	modern	modern
Precambrian basement aquifer (general)												
Hog82	Mentlatalet	B	5.5281	22.8094	−2.59	<DL	71.6	2.800	modern	modern	modern	modern
Hog84	Mentlatalet	B	5.3453	22.8569	−10.25	7.4	111.2	modern	modern	modern	modern	modern
Hog86	Selborak	B	5.0131	22.7907	−4.66	6.3	25.4	11.300	modern	2.300	3.800	3.000
Hog88	Tihigouine	B	5.50766	22.76636	−6.49	nd	79	1950	modern	modern	modern	modern
Hog91	Tihigouine	B	5.3453	22.765	−7.0	2.3	35.4	8.600	modern	modern	modern	modern
Hog96	Tadeddine	B	5.5008	22.5514	nd	8.7	106.2	modern	modern	nd	nd	nd
Hog100	Imedene	B	5.9178	22.6683	nd	8	96.8	270	modern	nd	nd	nd

Table 4
$^{87}Sr/^{86}Sr$ isotopic ratio, Rb and Sr concentration for Central Hoggar groundwaters.

ID	Localization	Rb (ppb)	Sr (ppb)	1/Sr mg/L	Rb/Sr	$^{87}Sr/^{86}Sr$	±Sd 2σ
Hog2t	Tazrouk	0.23	341	2.93	0.000681	0.709437	0.000009
Hog4	Idelès Palm	0.26	355	2.81	0.000741	0.707744	0.000008
Hog7	Hirafok	0.97	443	2.3	0.002178	0.710091	0.000007
Hog9	Tahifet	1.40	536	1.9	0.002621	0.712933	0.000008
Hog13	In-Amguel	0.71	591	1.7	0.001202	0.712879	0.000008
Hog69	Outoul	0.16	1329	0.75	0.000124	0.709492	0.000008
Hog5	Idelès-crater	32.33	29.7	33.7	1.089653	0.706386	0.000008
Hog30	Silet	0.01	494	2.02	0.0001	0.704099	0.000006
Hog30b	Silet	5.16	437	2.3	0.011809	0.704094	0.000006
Hog33	Silet	0.73	890	1.1	0.000822	0.704625	0.000007
Hog35t	Abalessa	0.32	717	1.4	0.000440	0.708418	0.000011
Hog16	Tahabort	80.5	316	3.16	0.254505	0.722298	0.000008
Hog42	Adriane	60.0	775	1.3	0.077408	0.714449	0.000010
Hog45	Pic Ihrarène (S)	36.5	948	1.05	0.038444	0.719602	0.000008
Hog70	Pic Ihrarène (N)	37.0	276	3.6	0.134235	0.719652	0.000010
Hog76	In-Kouf	0.91	905	1.1	0.001006	0.719407	0.000007
Hog77	Amsel	1.05	1105	0.9	0.000952	0.713887	0.000007
Hog78	Amsel	3.75	610	1.6	0.006151	0.712879	0.000008
Hog80	In-Zaouane	0.90	979	1.02	0.000914	0.717552	0.000009
Hog82	Metnatalet	0.99	703	1.42	0.001402	0.714942	0.000008
Hog83	Ihilfen	0.69	543	1.84	0.001279	0.708055	0.000007
Hog84	Outoul	0.43	343	2.91	0.001253	0.708011	0.000007
Hog86	Selborak	0.85	557	1.8	0.001527	0.709785	0.000010
Hog91	Tihigouine	1.27	732	1.37	0.001730	0.719529	0.000008
Hog92	Amsel	0.47	377	2.65	0.001243	0.713602	0.000008
Hog95	Tamanrasset (town)	0.50	1161	0.9	0.000434	0.719279	0.000010
Hog96	Tadeddine	0.56	276	3.62	0.002022	0.722811	0.000010
Hog97	Tifert	0.57	333	3.0	0.001727	0.706210	0.000012
Hog99	Outoul	0.20	362	2.77	0.000556	0.708519	0.000009
Hog100	Imedène	0.53	432	2.31	0.001229	0.721554	0.000008
Hog101	Tifouguinne	0.18	580	1.73	0.000313	0.716733	0.000011
Hog102	Ezernène	0.09	506	1.98	0.000172	0.709609	0.000008
Hog103	Afilal (guelta)	1.43	739	1.35	0.001935	0.705098	0.000007

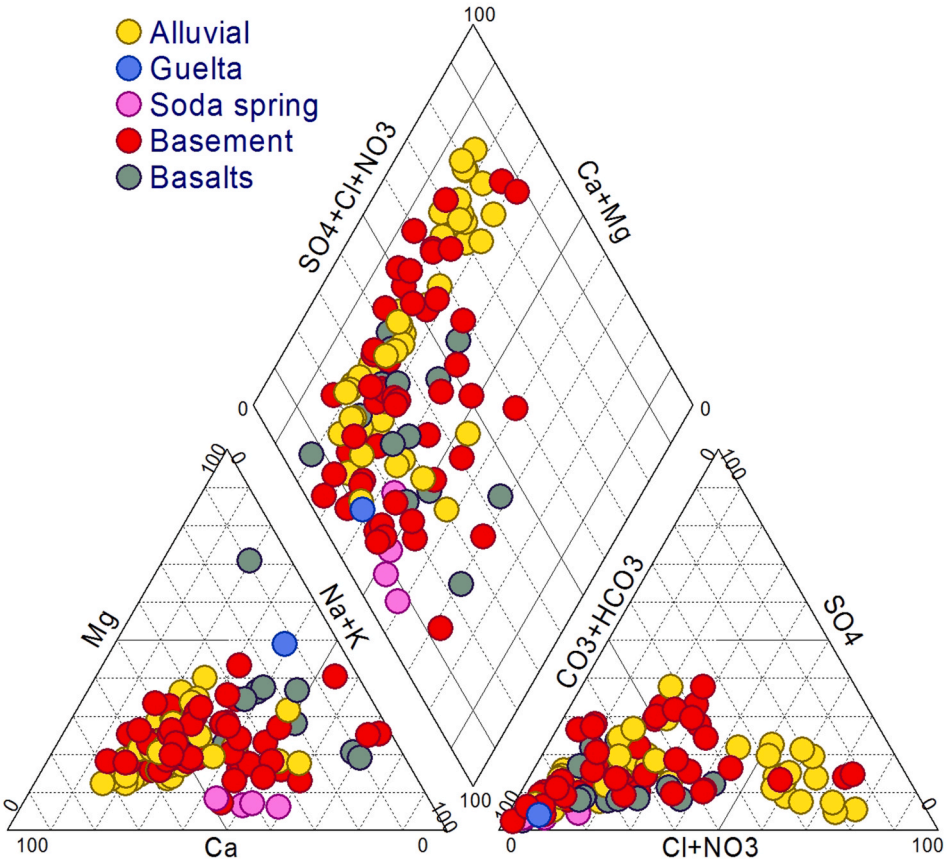

Fig. 4. Piper Diagram with the different hydrochemical facies.

are closed to the Global Meteoric Water Line (GMWL) and below the Local Meteoric Water Line (LMWL data from GNIP-IAEA/WMO, 2006, IAEA, 2005 at Assekrem station during 7 years observations, IAEA, 2008). Deuterium excess, *d*, calculated with a theoretical slope of 8 according to Dansgaard (1964) ranges for all the sampling points from −8.1 to 12‰ with an average value, excepting the evaporated waters (Table S1), around 9‰, identical to that found in rain water (9‰) at the Assekrem station (Saighi et al., 2001). The stable carbon isotopic composition $\delta^{13}C$ measured on 16 samples of the TDIC is reported in per mil (‰) relatively to the international standard Vienna-PDB (VPDB) and exhibit a wide range from −12.5 to −2.1‰. The depleted values (−12.5 and −11.7‰) are found in volcanic and alluvial aquifers for which the water level is near the surface (~12 mbgl) while the more enriched value is found in production wells in the ASZ and at Tahabort spring.

4.2.2. Radiogenic Sr isotopes

The Hoggar groundwater samples display $^{87}Sr/^{86}Sr$ ratios from 0.704 to 0.722 (Table 4). The lowest values are found in the Silet basaltic district and the highest values in the Tahabort soda spring near the Ediacaran In-Tounine sub-circular pluton and in a basement groundwater near the Ahelheg pluton, Ahelheg and In Tounine being twin plutons (Fig. 1b; Boissonnas, 1974; Azzouni-Sekkal et al., 2003) characterized by very high $^{87}Sr/^{86}Sr$ ratios (Table 4).

4.2.3. Radioactive isotopes

^{3}H activity range from 2.1 to 15.4 TU (measured for the last in 1997) for all the aquifers around the Hoggar. The lowest activity, 2.1 TU, is found at the Tahabort spring while the highest value is found in a well of Silet volcanic district (W of Tamanrasset). At Hog 103 (guelta Afilal ~2020 m elevation), 5.2 TU were found (in 2007). From the GNIP database of the Assekrem station, the weighted mean value of ^{3}H activity of rainwater was about ~13 TU in the mid-1990s. Taking into account the half-life of ^{3}H (which is 12.32 years), one can consider that the ^{3}H activity in rainwater nowadays should be about 2.5–3 TU or 4 TU, which corresponds to the results obtained for the groundwater of the region.

^{14}C activity is given in % of modern carbon (pMC) and was measured on TDIC of 18 groundwater samples (Table 3). ^{14}C values ranges from 0.2 to 117 pMC. The ancient pole is located along the ASZ and spring Tahabort while the modern pole is located in alluvial and Precambrian basement aquifers where the static level is near the surface.

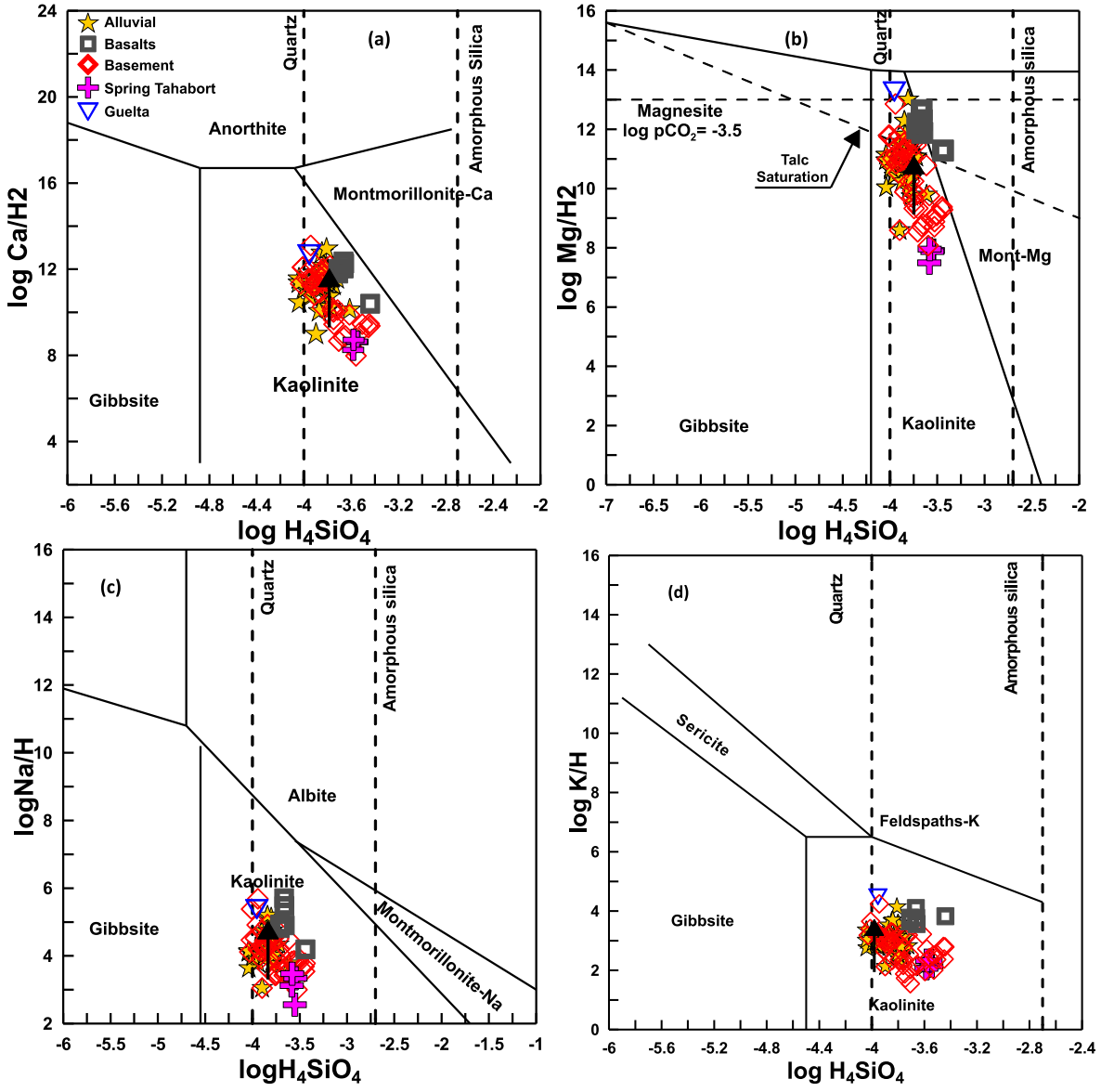

Fig. 5. Main stability diagrams for the volcanic, basement and alluvial aquifers.

5. Discussion

5.1. Groundwater in Precambrian basement

5.1.1. Close to ASZ and in other localities

In Central Hoggar desert area, the groundwater hydrochemistry is governed by the weathering and by the hydrolysis of the silicates. The main minerals constituting the granites and gneisses from the basement are mostly quartz, K-feldspar, plagioclase (Na–Ca feldspar), micas (muscovite and biotite), amphibole and pyroxene. In Cenozoic basalts, main minerals are olivine, nepheline, plagioclase, amphibole and pyroxene. Consequent alteration minerals are mainly kaolinite, montmorillonite, illite and chlorite. Hydrolysis increases Ca, Mg, Na and HCO_3 as well as silica (mainly as H_4SiO_4) according to the main following reactions (Edmunds, 1981; Appelo et al., 2005; White, 2005):

$$\underset{(Albite)}{2NaAlSi_3O_8} + \underset{soli\ Co_2}{2CO_2} + 6H_2O \rightarrow \underset{(Montmorillonite)}{Al_2Si_4O_{10}\ (OH)_2} + 2Na^+ + 2HCO_3 - + 2H_4SiO_4 \quad \text{(Eq.3)}$$

$$\underset{(Biotite)}{KM_{g3}AlSi_3O_{10}\ (OH)_2} + 7H_2CO_3 + 0.5H_2O \rightarrow K^+ + 3Mg^{2+} + 7HCO_3 - + 2H_4Sio_4 + 0.5\underset{(Albite)}{AlSio_2O_5\ (OH)_4} \quad \text{(Eq.4)}$$

$$\underset{(Mica,\ Muscovite)}{3KAlSi_3O_8} + 2H_2CO_3 + 12H_2O \rightarrow 2K^+ + 2HCO_3 - + 6H_4Sio_4 + \underset{(Orthose)}{KAlSi_3O_{10}\ (OH)} \quad \text{(Eq.5)}$$

$$\underset{(Anorthite)}{CaAl_2Si_2O_8} + H^+ + H_2O \rightarrow \underset{(Kaolinite)}{Al_2Si_2O_5(OH)_4} + Ca^{2+} \quad \text{(Eq.6)}$$

These reactions induce a production of silicic acid (H_4SiO_4) with a release of HCO_3^- at high concentrations. In the ASZ, a high pCO_2 (0.1006–1.0576) and low pH (5.82–6.8) has been measured (Table 1). The Al released from the weathering of the primary silicate is incorporated in a secondary phase and the stability between the two minerals is controlled by the available silicic acid produced (dissolved silica) and by the other released products Ca, Mg Na and K (Appelo et al., 2005). In the resulting silicate mineral stability diagrams (Fig. 5), the studied samples are all located within the stability field of the kaolinite, either the Na and K-rich phases or the Ca–Mg phases. In the metastable domain, all the points fall in the quartz field. The sample composition variability is small for Na and K (Fig. 5c and d) and higher for Ca and Mg. This may indicate that the main hydrolysis process in the presence of carbonic acid (H_2CO_3) is primarily close to the Na and K poles (sodic plagioclase and K-feldspar). Whatever, in the Hoggar groundwater hydrosystem, kaolinite is by far the most stable secondary silicate phase.

Outside the ASZ, the Hoggar groundwaters are globally undersaturated with respect to the main minerals as well as to calcite, gypsum, halite, anhydrite and strontianite. Within the shear zone, they are in equilibrium or saturated regarding the same minerals (Table S4; Fig. S6). Weathering of silicates in the Hoggar mountains is controlled (Eq3-6) by the uptake of CO_2 while HCO_3^- abundance is related to the cation concentrations (Na, K and Ca). The deepest groundwaters (basement aquifers) and those corresponding to the ASZ have the highest Na^+ and HCO_3^- content (Table 1; Fig. 6a): e.g., the water close to the Adriane trachyte lava has [Na] ≫4 mMol/L (Table S1). One sample (Hog5 in Idelès crater) is particularly rich in Mg ([Mg] >6.8 mMol/L). The correlation between $[HCO_3]$ and ([Na]+[Ca]+[Mg]) is poorly defined (Fig. S2b) except for the alluvial groundwaters that fall near or around the equiline 1:1. This indicates that the alkalinity of alluvium waters is related to these basic cations. The samples located to the right of the equiline belong mainly to the shear zone area, suggesting that their alkalinity could be related to geogenic CO_2 influx moving along the shear zone. This can be correlated with the fluids located along Hoggar shear zones evidenced by magneto-telluric data (Bouzid et al., 2015).

Considering the proportions obtained by the hydrogeochemical modeling, the five points close to the ASZ have $H_2CO_3 \geq HCO_3^-$ (H_2CO_3: 57% to >76%), revealing a low pH, whereas the other Hoggar samples have $HCO_3^- \geq H_2CO_3$ (HCO_3^-: mean value of 86%). All the points are to the left of the calcite dissolution line (2 $[Ca^{2+}] = [HCO_3^-]$), indicating that calcite dissolution cannot be the main process in the HCO_3^- acquisition, whether it is the Adriane shear zone or the other aquifers (Fig. 6a; Schofield and Jankowski, 2004). Alkalinity has a >50% influence in the anion budget and plays an important role in the groundwater hydrochemistry (Fig. 6b). This is related to a silicate weathering slower than the CO_2 hydration and dissociation to HCO_3^- (Appelo et al., 2005; Schofield and Jankowski, 2004). However, for the samples located in the ASZ, the DIC is much higher than the alkalinity (DIC/ALK = 2.3 to 4.6 mMol/L), which is not the case elsewhere in the Hoggar (mean value of 1.4 mMol/L). DIC and ALK can thus be used to decipher the reactions that contribute to the CO_2 in the hydrosystem (Stumm and Morgan, 1996; Schofield and Jankowski, 2004). In Fig. 6b, some samples are located well to the right of the 1:1 line, meaning that the DIC entering the system is by far in excess over ALK and all these samples belong to the shear zone. Elsewhere, samples have values close to unity. For the latter, the equilibrium was reached, while for the waters with DIC/ALK ratio ≫1, the system can be considered as open to geogenic CO_2 (Table 1, Fig. 6b). Near the Adriane trachyte lava, the DIC origin of five samples (1 spring-Hog16 and 4 boreholes tapping the basement) can be linked to H_2CO_3 related to the continuous influx of deep CO_2 that is recorded in the Tahabort soda spring (Hog16), also located on the ASZ.

Additional information on the evolution of the other major anions and cations and trace elements can be found in the supplementary material.

5.2. Isotopic constraints

5.2.1. Stable isotopes

Central Hoggar is mainly influenced by two types of precipitations: (i) those coming from the Polar Front and from the Mediterranean basin during the minor rainy season from November to April, which has stable isotope depleted weighted mean value ($\delta^{18}O = -4.6‰$, $\delta^2H = -19‰$ vs VSMOW) and (ii) those coming from the Inter Tropical Front (ITF), during the summer main rainy monsoon season from May to October, which has different stable isotope weighted mean value ($\delta^{18}O = -2.5‰$, $\delta^2H = -14.3‰$ vs VSMOW). The Hoggar groundwater recharge depends on these meteoric waters that occur during brief but often intense storms and are affected by an intense evaporating process.

Alluvial groundwaters in the vicinity of Tamanrasset (z = 1360 m. a. s.l) ($n = 23$) plot along a line with a slope of 2.58 while the groundwaters from the other Hoggar peripheral alluvial aquifers and those ($n = 7$) and those from Precambrian production wells, near or outside of the ASZ, ($n = 22$) extend along the LMWL (Fig. 7a). This indicates that the latter are also affected by an evaporation process.

Three production wells (d~100m), located in the ASZ, have seen

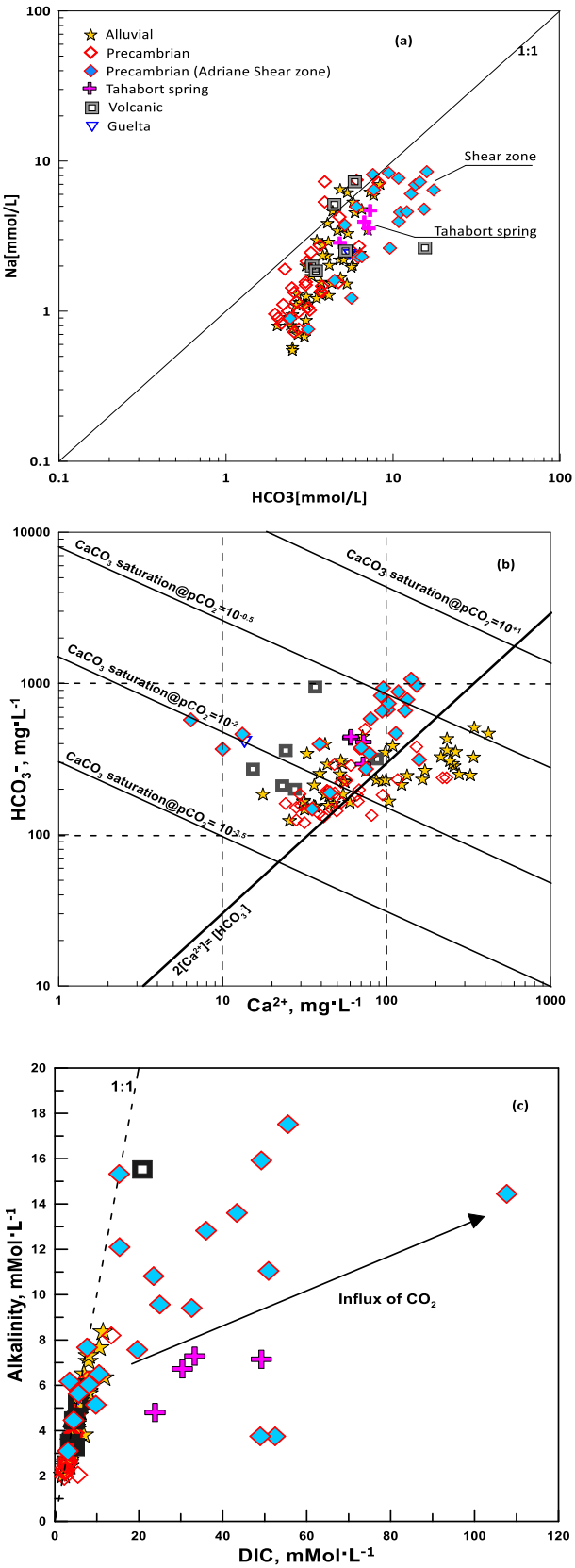

Fig. 6. (a) Na–HCO_3 binary evolution diagram; (**b**) Modified from Stumm and Morgan, (1996): Evolution of the groundwater alkalinity in the Central Hoggar with respect to Ca^{2+} and (**c**) Alkalinity vs DIC (Dissolved Inorganic Carbon) showing the particular character of the deep groundwater in the shear zone. (Symbols are the same like for Fig. 6).

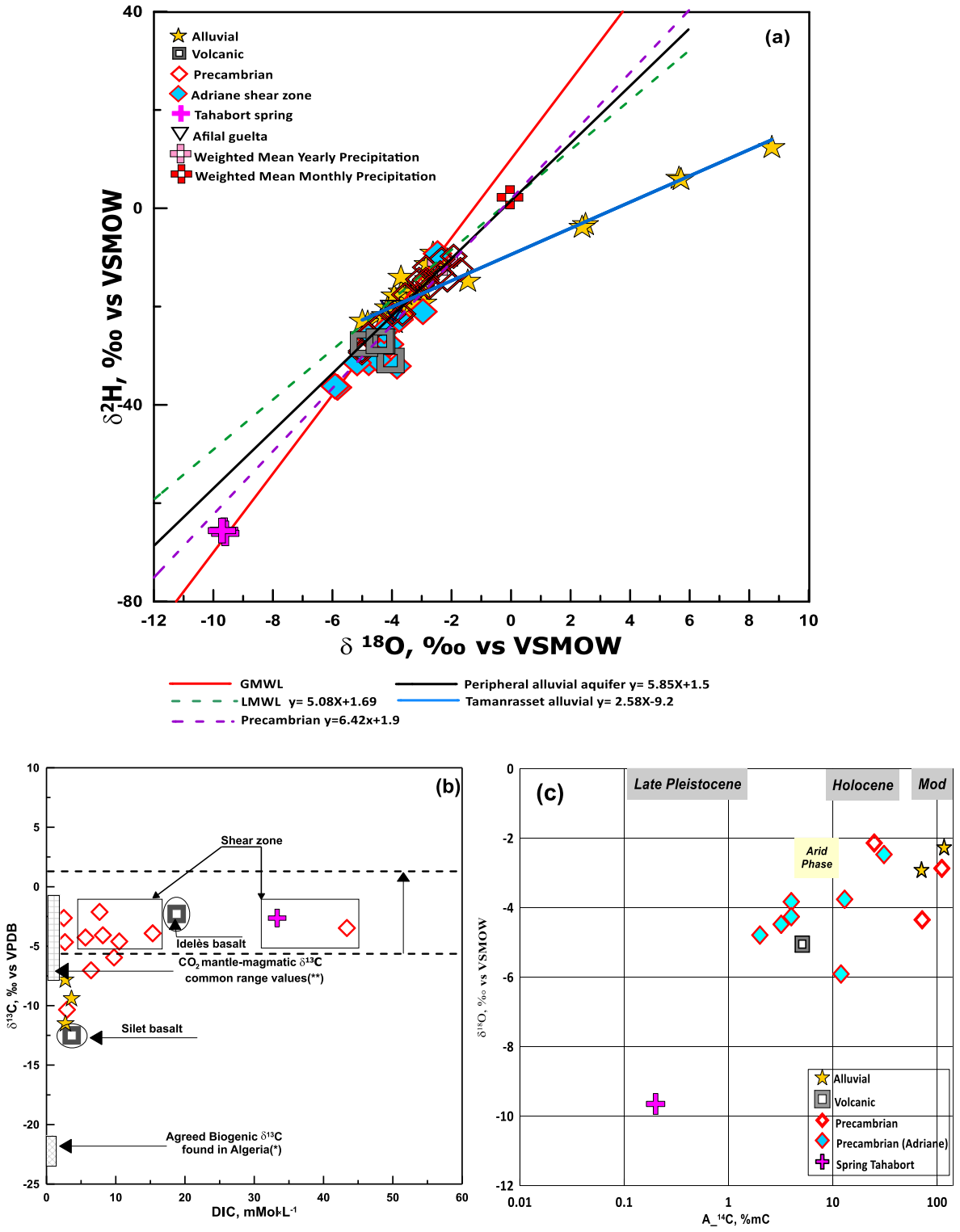

Fig. 7. (a) Stable Isotopes distribution of the alluvial and basement aquifer. The weighted means (yearly, major and minor) of precipitation values taken from the Assekrem pluviometric station (GNIP, IAEA/WMO, 2006) are given for comparison. (b) Hoggar GW δ^{13}C-DIC variations (Symbols are the same like for Fig. 6) and (c) δ^{18}O-a_^{14}C relation (symbols are the same like for Fig. 6).

their isotopic content to change during the three years of sampling. While in 2002 they were aligned along a line with a slope of 5.33, in 2004 they were aligned along a line indicating an enrichment in δ^{18}O suggesting a more important water-rock interaction. This was confirmed by a rapid deterioration of the hydrochemical features of these bores with a rapid increase of SC and alkalinity, high pCO_2 and H_2S odor. In 2007, their isotopic content went back to their initial values. These variations in isotope contents could be explained by variations in the fluid movements along shear zones delineated by magneto-telluric measurements (Bouzid et al., 2015). The overall isotopic signature of these waters corresponds to that of rainfall which has undergone evaporative enrichment before or during infiltration through the

alluvium deposit (Gonfiantini et al., 1974; Fontes et al., 1986).

The natural soda spring Tahabort (Hog16), emerging from the Adrar Ihagaren-In Tounine batholith (Azzouni-Sekkal et al., 2003) near the Adriane trachytic lava, exhibits $\delta^{18}O$ mean of −9.6‰ and $\delta^{2}H$ values mean of −65.7‰ vs V-SMOW (Fig. 7a). These values, recorded during three different periods and corresponding to that of Saighi (1999) are strongly depleted but stand on the lower part of the GMWL line (Fig. 7a). This indicates that the Tahabort spring soda water is inherited from an ancient pluvial period with very different specifications than the present period. Tahabort Spring values represent a cold-water pole with a high residence time corresponding to a more humid and colder paleoclimatic period.

The homogeneity of most of the samples can be attributed to the topography, which does not favor persistence of waters at the surface (with the exception of rare gueltas) and to the well-developed fracture network in the Precambrian basement. Both features favor a fast infiltration of the precipitations and their concentration either in the alluvial reservoirs of limited surface or in the volcanic or Precambrian aquifer systems where fractures are developed and, as a consequence where rocks are weathered. This supports homogenization of water composition within each type of aquifers.

The fact that the large majority of the samples lie on or very close to the GMWL and LMWL means that these waters were first influenced by local rain and condensing vapor incursion coming from the Atlantic Ocean and then by the Sudanese-Saharan monsoon (ITF). Indeed, the deuterium excess, *d*, has an average value of 9‰ ($n = 74$) close to that of the GMWL value of 10‰. At Assekrem station, deuterium excess values of 2–10‰ are observed for summer rains and greater values (10–20‰) for winter rains (Saighi, 2005), revealing both the Atlantic and monsoon influences.

5.2.2. *Tritium content*

Tritium (^{3}H) content in recent precipitations is not available for Hoggar. We thus took as a reference the ^{3}H values measured in the mid-1990s at Assekrem station that are ~ 13 TU (1TU = 0.119 Bq/L). This value falls within the natural tritium nowadays (8–15 TU; Cauquoin et al., 2015). ^{3}H has been measured on 22 samples from the 3 types of aquifers, three samples having values below the detection limit (Table 1). The highest value is found in the volcanic aquifer (15.4 TU) and a high value in the alluvial aquifer (8.6 TU). The lowest values, below the detection limit, are found in the three types of aquifers. ASZ boreholes have TU from 1.2 to 3.5, with a well at 6.9 TU. Outside the ASZ zone, boreholes have value from 2.3 to 8.7 TU. The Afilal guelta has a value of 5.3 TU and the Tahabort spring a value of 2.1, among the lowest ones measured.

The Hog30 (volcanic aquifer) value of 15.4 TU can be considered as corresponding to the modern rain, measured at Atakor station (13 TU). All the other measured values are lower and imply the input of water with some residence time at depth, where the tritium decays (half-life of ^{3}H: 12.32y) with no new production. 25 years is enough to bring ^{3}H to 3–4 TU, which is the mean value in the Precambrian aquifers. However, it is likely that all these aquifers are filled by a mixing of recent rainwater and water with residence time >25 years, precluding to calculate a residence time with tritium.

5.2.3. *Carbon isotopes ($\delta^{13}C$-DIC, ^{14}C-DIC)*

In arid zones, like Central Hoggar, $\delta^{13}C$ can vary significantly. This variation can be modeled through a geochemical exchange between atmospheric and geogenic CO_2 (Clark and Fritz, 1997, p211). In Central Hoggar, Hog16 (Tahabort soda spring; $\delta^{13}C = -2.64$‰ vs VPDB) can be taken as the geogenic pole, i.e., deep water with high residence time and Hog30 (dug well in the Tahalra basalt district with a tritium content similar to rainwater; $\delta^{13}C$ of −12.5‰ vs PDB) can be adopted as the atmospheric pole, i.e., the water recharge value. With these two references, we can correct the ^{14}C activities and appreciate the residence time i.e., the time that elapsed since the water is underground (Table 3,

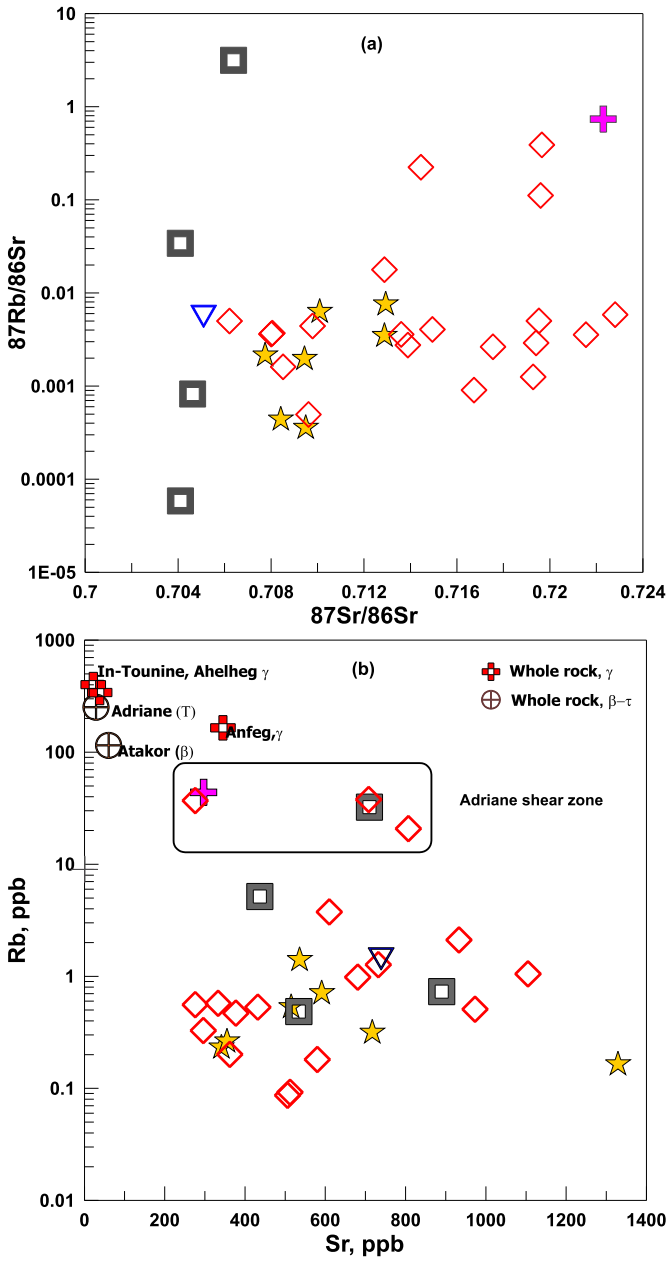

Fig. 8. (a) $^{87}Rb/^{86}Sr$ vs $^{87}Sr/^{86}Sr$ and **(b)**: Rb vs Sr (in both whole rock and groundwaters to see the extent of the water-rock interaction) showing the peculiar character for some points in the shear zone.

Fig. 7c). The two q calculated factors (Table 3) do not differ from each other due to the very small difference calculated between $\delta^{13}C_{Soil\text{-}CO2}$ and $\delta^{13}C_{rech}$, which in the present case can be rounded to −21‰. This is consistent with what has been found in previous studies in Algeria (Guendouz, 1985) and what is applied in semi-arid to arid zones (Clark and Fritz, 1997, Cartwright et al., 2020; Simler, 2020).

Ten samples provide modern values and have thus a short residence time that cannot be specified. Eight samples provide old ages (between 3000 and > 30,000 years) among which five can be considered as fossil waters (>12,000 years; Ferguson et al., 2020).

The older fossil water is emerging at Tahabort spring (Hog16) along the ASZ. With its A_o <0.2pMC, it is at the limit of the method (i.e., >30 ka), in agreement with the $\delta^{18}O$ and $\delta^{2}H$ indicating a cold pole with high strontium radiogenic isotope (see below). Its ^{3}H concentration >0 (2.1 TU) indicates that recent water mixed with the fossil water with a proportion of c. 15% implying that the age obtained is a minimum age for

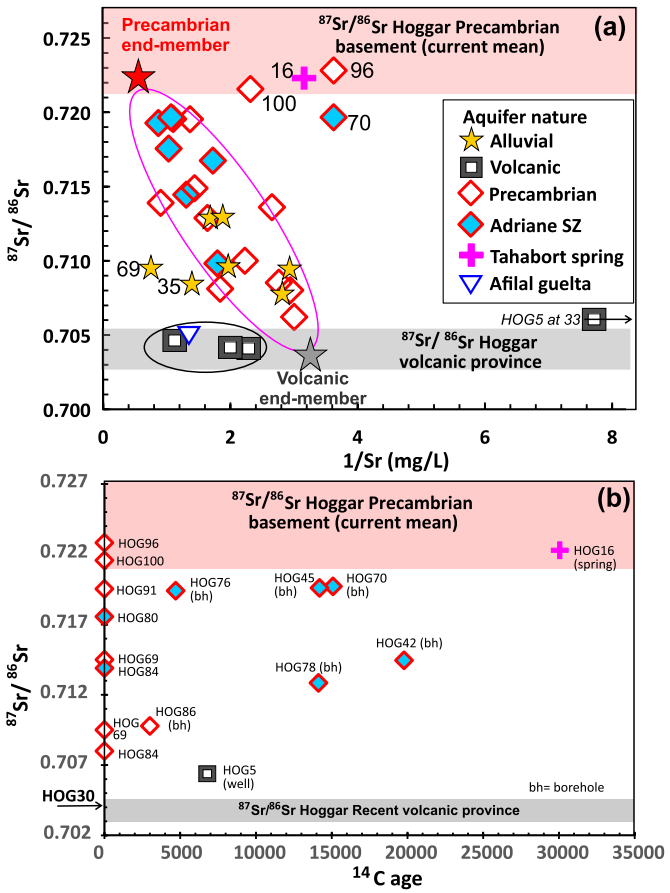

Fig. 9. (a) $^{87}Sr/^{86}Sr$ vs 1/Sr for Hoggar groundwaters; (b) $^{87}Sr/^{86}Sr$ vs ^{14}C ages.

the old component. Three other fossil waters are found in Hog42, 45 and 70 (19.8 ka, 14.2 ka and 15 ka, respectively), located along the axis of the ASZ, not far from the Tahabort soda spring. The fifth fossil water (Hog78; 14.1 ka) is located to the south slightly to the east of the ASZ, suggesting that it is located on a satellite fault of the latter. Their ^{3}H contents, 1.7, 2.3, 1.2, 3.5 TU respectively, indicate also a mixing with modern recharge water, with a proportion of 8–23%. Older recharges than a few tenth of years cannot be estimated, indicating also that the above ages are minimum ages. On the other hand, the presence of geogenic CO_2, by definition devoid of ^{14}C, could increase the calculated residence times, especially at Tahabort spring.

Although located close to Hog 78, the production well Hog 76 gave a significantly younger residence time (4.7 ka). The dug well Hog5 (with high TDS, pCO_2, and alkalinity) is located 135 km northward but in the continuity of the ASZ and gave also an old age (6.79 ka). Both samples have tritium content below the detection limit (Table 1) indicating the absence of mixing with recent water. This does not preclude mixing with surface water beyond the tritium oversight but at the very least this indicates a minimum residence time of 5–7 ka for the old Hoggar water. This is in agreement with data coming from Hog 86 sample, which is located far to the west, between Tamanrasset and Silet: it gives a residence time of 3 ka, which if considering 40% of modern water as indicated by tritium (6.3 TU), can be corrected to 5 ka.

However, residence times of c. 15 ka suggested by the oldest ages obtained, are likely in Hoggar. Indeed, both to the north and to the south of Hoggar, in the Eastern erg sub-basin (NE of Hoggar, Guendouz et al., 1998) and in the Irghazer plain (SE of Hoggar, Andrews et al., 1994), noble gas recharge MAAT (mean annual air temperature) of c. 16.9 °C is found 15 ka ago, i.e., c. 5 °C lower than the present mean temperature. Colder MAAT temperatures (14.5–17.6 °C, which is c. 8 °C lower than now) have also been determined for 15 ka ago in the Khrechba field oil (800 km north of Hoggar; Darling et al., 2018). On the other hand, global patterns of late-glacial to late-Holocene precipitation ^{18}O shifts suggest that stronger isotopic distillation of air masses than now prevailed during this period due to larger differences in temperature between the tropics and the poles (Jasechko, 2015). These colder temperatures can explain the depleted values in $\delta^{18}O$ and $\delta^{2}H$, found at Tahabort spring.

5.2.4. *Source of radiogenic $^{87}Sr/^{86}Sr$ in the Hoggar groundwaters*

The large contrast in age and in Rb/Sr ratios between Precambrian basement and the Cenozoic mantle volcanic rocks makes strontium isotopes an excellent tracer for Hoggar groundwaters. In Hoggar ground and surface waters (guelta), there is no correlation between $^{87}Sr/^{86}Sr$ and $^{87}Rb/^{86}Sr$ ratios (Fig. 8a) or between Rb and Sr concentrations (Fig. 8b). This indicates a decoupling of the sources of Rb and Sr and/or a different behavior of Rb and Sr during the alteration process of minerals induced by water.

In the diagram 1/Sr vs $^{87}Sr/^{86}Sr$ (Fig. 9a), where mixing processes determine straight lines and not curves, most of the basement and alluvial waters extend between two end-members located in the Precambrian basement signature and in the Cenozoic volcanic province signature, respectively. The Precambrian end-member is radiogenic and enriched in Sr ($^{87}Sr/^{86}Sr = 0.721$ and 1800 ppb Sr) and the Cenozoic volcanic end-member is unradiogenic and poor in Sr ($^{87}Sr/^{86}Sr = 0.704$ and 270 ppb Sr). Let us note that the values of these end-members are close to the two tips of the sample trends and are only slightly extrapolated. In addition, some water samples have similar $^{87}Sr/^{86}Sr$ ratios than those inferred for the end-members although with different Sr concentrations (see below). So, these two end-members can be considered as well constrained. The water basement end-member is characterized by a higher Sr content (c. 1800 ppb) than that of the water volcanic end-member (c. 270 ppb). This can be related to the higher abundance of Sr-rich minerals in the basement, especially biotite, a mineral prone to release Sr during weathering (Taylor et al., 2000) and to a higher alteration of the Precambrian basement relatively to the Cenozoic volcanic one. The trend observed between the two end-members implies that the waters apparently emerging from the Precambrian basement have a partial, sometimes predominant, volcanic signature, which was not expected. The most likely explanation is that these waters follow faults coated by volcanic products with no remnants at the surface. This supports the existence of ubiquitous volcanic fluids along the shear zones of the Hoggar as concluded by Bouzid et al. (2015) on the basis of magneto-telluric data.

Waters from the Tahalra volcanic district aquifers (Hog 30, 30b, 33, 97; Fig. 2), with low $^{87}Sr/^{86}Sr$ (0.704–0.706), have higher Sr contents (400–900 ppb) than the water volcanic end-member (270 ppb) showing that a direct contact with the volcanic rocks can generate high Sr contents in water, confirming the major role played by the alteration of the Sr-rich minerals. The Hog5 sample, taken in the Idelès crater, has a low, volcanic type, $^{87}Sr/^{86}Sr$ ratio (0.7064) but a very low Sr content (30 ppb). This can be related to a stationary water in the crater unable to exchange significantly with the country-rocks. The Afilal guelta has the same signature as the volcanic aquifer waters.

The lower Sr content of the water volcanic end-member determined by the basement aquifers relatively to water in direct contact with the basalts implies a different nature of the volcanic products represented by this volcanic end-member. In the trend pointing to the two waters end-members, waters situated in the Adriane shear zone are, as a mean, closer to the Precambrian water end-member than the waters coming from the other Precambrian sites (Fig. 9b). This can be linked to several causes not mutually exclusive: (1) this still working major fault (Liégeois et al., 2005) has partly destroyed the volcanic varnish present along it, enhancing the contact with the tectonized Precambrian basement, by contrast to more minor faults; (2) this is related to the nature of the volcanic products at depth, containing less Sr-rich minerals, generally late in the crystallization sequence; (3) these aquifers are more easily

replenished with rainwater, being very low in Sr as in all elements. A major point imposed by this trend is that all these waters are circulating along faults that were used by volcanism for outpouring lavas.

In addition, the fact that the volcanic end-member Sr content determined by the basement waters does not correspond to that of the water present in the volcanic area implies that the trend determined by the basement waters do not result from the mixing between "volcanic" water and "basement water" but results from local and variable interaction with volcanic and Precambrian products in the conduits. This indicates that the aquifers are linked to shear zones and faults and do not develop laterally.

Four waters (Hog16, 70, 96, 100) have high $^{87}Sr/^{86}Sr$ ratios (0.7197–0.7228) but lower Sr contents (275–430 ppb) than the inferred basement end-member (>900 ppb) i.e. 1/Sr between 2 and 4 rather than <1 (Fig. 9a). This could be related to areas where basement rocks are less altered and are delivering less Sr, suggesting that these waters are located outside of faults where volcanic products are present and where Precambrian rocks are tectonized and more prone to deliver Sr. This is the case of Hog96 and Hog100 located much more to the east (Fig. 2), and of Hog70, from the Tahabort soda spring where CO_2 is present, rendering the water sparkling. The origin of this gas is not known but it could change the interaction between the water and its country-rocks. More data are needed to constrain this particular environment. Hog70 is located in the ASZ and no explanation can be given for its low Sr content. This does not seem to be linked with the duration of contact with the country-rocks, this sample has a relative high resident age (15 ka; Fig. 9b). Globally, these four waters have variable resident time, from modern to 30,000 years (Fig. 9b). This diagram shows that nearly all old waters are located in the ASZ and collected from boreholes. Only Hog5 comes from a well and Hog16 from a spring probably linked to deep structures (CO_2-rich water).

The plot of ^{14}C ages against $^{87}Sr/^{86}Sr$ (Fig. 9b) shows no correlation between ^{14}C ages and $^{87}Sr/^{86}Sr$ ratios, indicating that the acquisition by water of their Sr isotopic ratio is fast. This means that waters reach rapidly equilibrium with country-rocks as far as $^{87}Sr/^{86}Sr$ ratios are concerned, implying that the water-rock interactions in groundwaters are geographically limited and linked to geological structures, indicating also the existence of independent aquifers. We can distinguish at least three different aquifers: (1) an aquifer along the ASZ, (2) an eastern aquifer close to the In-Tounine and Ahelheg plutons, (3) an aquifer linked to shear zones coated by Cenozoic basalts in the Silet district (Tahalra terrane).

6. Conclusion

- In Central Hoggar, three main types of aquifers exist, within the alluvions, within the Cenozoic volcanic basement and within the granite-gneiss Precambrian basement. In addition, a major role is devoted to the Adriane shear zone (ASZ) that runs NE-SW just to the east of the main Hoggar town, Tamanrasset.
- In the Hoggar groundwater hydrosystem, kaolinite is by far the most stable secondary silicate phase resulting from the hydrolysis of basement minerals. Within the ASZ, groundwater is in equilibrium with the main rock minerals as well as with calcite, gypsum, halite, anhydrite and strontianite while outside the ASZ, they are undersaturated to the same minerals.
- Hoggar groundwaters are Na–HCO_3 type, with high pCO_2 and high HCO_3^- and SiO_2 concentrations. The deepest groundwaters (basement aquifers) and those in the ASZ have the highest Na^+ and HCO_3^- content. This is attributed to ascending geogenic CO_2 along shear zones interacting with Na feldspar. Geogenic CO_2, in its dissolved form, accounts for ~63% of the composition of TDIC concentration in deep wells while in the other alluvial, volcanic and Precambrian aquifers localities it represents only ~15% of the TDIC. The $\delta^{13}C$ content of TDIC increases progressively as deep geogenic CO_2 contributes to dissolve HCO_3^-. The water point, with the highest geogenic content, which is also the water with the highest residence time (>30 ka) is the Tahabort spring, a natural sparkling Na-rich source, located on the ASZ.
- A large number of water points (dug well or production well) are located along the ASZ and all waters with high residence time (3 ka to > 30 ka) are among them. The ASZ is, to this day, the only vector of deep and ancient water flows. Fossil waters derive from ancient rainy periods at 15 ka whose climatic characteristics were totally different from those of today
- Tritium values indicate that most of the waters from the Precambrian basement are the result of the mixing of recent rainwater and older waters (>100 years) in various proportion, the minimum participation of recent rainwater being 8%. On the other hand, recent or older, all these waters would result from local evaporated precipitation as shown by stable isotopes being most often close to the GMWL and LMWL.
- Trace elements have shown that waters in the Adriane shear zone are different from the other domains and are more concentrated in Rb, Sr, Cs, U, Ba, while the other aquifers are less affected by elevated concentration in toxic elements. In general, all the samples respect the WHO drinking guide lines and show concentrations lower than the MAC.
- Sr isotopes show that most of the studied samples lie on a unique trend between a Precambrian radiogenic end-member enriched in Sr ($^{87}Sr/^{86}Sr = 0.721$ and 1800 ppb Sr) and a non-radiogenic Cenozoic volcanic end-member poor in Sr ($^{87}Sr/^{86}Sr = 0.704$ and 270 ppb Sr). However, much of the waters extracted from the Precambrian basement have an unexpected significant volcanic signature implying that faults where water moves are largely coated by volcanic products. The latter deliver less Sr than the volcanic rocks themselves. As a whole, $^{87}Sr/^{86}Sr$ ratios show the existence of several aquifers linked to major faults and shear zones, among which the Adriane shear zone is the most prominent. This situation can be related to the metacratonic nature of the Precambrian basement (LATEA metacraton), rigid but fractured and invaded by recent volcanism (Liégeois et al., 2013; Brahimi et al., 2018).

Funding

This research did not receive any specific grant from funding agencies in the public, commercial, or not-for-profit sectors. This work was supported by the Government of Algeria through the Algiers Nuclear Research Centre (CRNA).

CRediT authorship contribution statement

M.E.H. Cherchali: Conceptualization, Field sampling, Data curation, Formal analysis, Methodology, Writing – original draft, Writing – review & editing. **J.P. Liégeois:** Conceptualization, Data curation, Formal analysis, Supervision, Validation, Writing – review & editing. **M. Mesbah:** Conceptualization, Field sampling, Data curation, Supervision, Validation, Writing – review & editing. **N. Daas:** Conceptualization, Data curation, Formal analysis, Methodology. **K. Amrous:** Conceptualization, Field sampling, Data curation. **S.A. Ouarezki:** Conceptualization, Data curation, Formal analysis.

Declaration of competing interest

The authors declare that they have no known competing financial interests or personal relationships that could have appeared to influence the work reported in this paper.

Acknowledgements

The authors are indebted to the local water authorities (Tamanrasset Water Resources Directorate) for providing all technical means to make possible the field sampling campaigns. The first author acknowledges the IAEA for training and makes possible the strontium analysis in the RMCA isotope laboratory (Tervuren, Belgium) through the TC project ALG/8/012. A special mention goes to the staff, both the present and retired ones, of the Dating and Isotope Tracing Department for their constant help and support during field and laboratory work. Sincere thanks go to the colleagues of the Tamanrasset Nuclear Research Centre for their great logistical support during the field missions. Many thanks to the associate editor Mr. Ian Cartwright as well as the three anonymous reviewers who by their interesting comments and advices have undoubtedly improved the quality of the manuscript. The study was supported by the Algiers Nuclear Research Centre.

Appendix A. Supplementary data

Supplementary data to this article can be found online at https://doi.org/10.1016/j.apgeochem.2021.105179.

References

Abdallah, N., Liégeois, J.P., De Waele, B., Fezaa, N., Ouabadi, A., 2007. The Temaguessine Fe-cordierite orbicular granite (Central Hoggar, Algeria): U–Pb SHRIMP age, petrology, origin and geodynamical consequences for the late Pan-African magmatism of the Tuareg shield. J. Afr. Earth Sci. 49, 153–178. https://doi.org/10.1016/j.jafrearsci.2007.08.005.

Abdeslam, M.G., Liégeois, J.P., Stern, R.J., 2002. The Sahara metacraton. J. Afr. Earth Sci. 34, 119–136. https://doi.org/10.1016/s0899-5362(02)00013-1.

Acef, K., Liégeois, J.P., Ouabadi, A., Latouche, L., 2003. The Anfeg post-collisional Pan African High-K calc-alkaline batholith (Central Hoggar, Algeria), result of the Latea micro continent metacratonisation. J. Afr. Earth Sci. 37, 295–311. https://doi.org/10.1016/j.jafrearsci.2003.10.001.

Andrews, et al., 1994. The evolution of alkaline groundwaters in the Continental Intercalaire aquifer of Irhazer Plain, Niger. Water Resour. Res. 30.

A.N.R.H. (Agence Nationale des ressources Hydriques), 1992. Notice explicative de la carte hydrogéologique du Hoggar et des Tassili, au 1/1.000.000, 1992. Projet PNUD, Janvier. ALG/88/021.

Appelo, C.A.J., Postma, D., 2005. Geochemistry, Groundwater and Pollution. https://doi.org/10.1201/9781439833544. A.A.Balkema/Rotterdam/Brookfield.

Azzouni-Sekkal, A., Bonin, B., Benhallou, A., Yahiaoui, R., Liégeois, J.P., 2003. Cenozoique Alkaline Volcanism of the Atakor Massif, Hoggar, Algeria. Geological Society of America. https://doi.org/10.1130/2007.2418(16.

Bendaoud, A., Ouzegane, K., Godard, G., Liégeois, J.-P., Kienast, J.-R., Bruguier, O., Drareni, A., 2008. The Eburnian Granulitic Metapelites of Tidjenouine, geochronology and metamorphic P- T-X evolution: witness of the LATEA metacratonic evolution (Central Hoggar, Algeria) from. In: Ennih, N., Liégeois, J.-P. (Eds.), The Boundaries of the West African Craton, vol. 297. *Geological Society, London*, Special Publications, pp. 111–146. https://doi.org/10.1144/sp297.6.

Beuf, S., Biju-Duval, B., de Charpal, O., Rognon, P., Gariel, O., Bennacef, A., 1971. Les grès du Paléozoïque inférieur au Sahara. Sédimentation et discontinuités. In: Evolution structurale d'un craton. Publication Institut Français du Pétrole, Collection Science et Techniques Pétrolières, vol. 18. Editions Technip, Paris, p. 464.

Black, R., Latouche, L., Liégeois, J.P., Caby, R., Bertrand, J.M., July 1994. Pan-African displaced terranes in the Tuareg shield, (Central Sahara). Geology 22, p641–644. https://doi.org/10.1130/0091-7613(1994)022%3c0641:padtit%3e2.3.co;2.

Boissonnas, J., 1974. Les granites à structures concentriques et quelques autres granites tardifs de la chaîne pan-africaine en Ahaggar (Sahara central, Algérie). Thèse, Centre de Recherches sur les Zones Arides. Ser. Geol. 16, 662.

Bouzid, A., Bayou, B., Liégeois, J.-P., Bourouis, S., Bougchiche, S.S., Bendekken, A., Abtout, A., Boukhlouf, W., Ouabadi, A., 2015. Lithospheric structure of the Atakor metacratonic volcanic swell (Hoggar, Tuareg Shield, southern Algeria): electrical constraints from magnetotelluric data. In: Foulger, G.R., Lustrino, M., King, S.D. (Eds.), The Interdisciplinary Earth: A Volume in Honor of Don L. Anderson, vol. 514. Geological Society of America Special Paper, pp. 239–255. https://doi.org/10.1130/2015.2514(15.

Brahimi, S., Liégeois, J.-P., Ghienne, J.-F., Munschya, M., Bourmatte, A., 2018. The Tuareg shield terranes revisited and extended towards the northern Gondwana margin: magnetic and gravimetric constraints. Earth Sci. Rev. 185, 572–599. https://doi.org/10.1016/j.earscirev.2018.07.002, 2018.

Burgeap, 1975. Mission d'expertise hydrogéologique dans le Hoggar. Sonarem, Alger.

Cartwright, I., Currell, M.J., Cendón, D.I., Meredith, K.T., 2020. A review of the use of radiocarbon to estimate groundwater residence times in semi-arid and arid areas. J. Hydrol. 580 https://doi.org/10.1016/j.jhydrol.2019.124247, 2020.

Cauquoin, A., Jean-Baptiste, P., Risi, C., Fourré, É., Stenni, B., Landais, A., 2015. The global distribution of natural tritium in precipitation simulated with and Atmospheric General Circulation Model and comparison with observations. Earth Planet Sci. Lett. 427, 160–170. https://doi.org/10.1016/j.epsl.2015.06.043, 2015.

Cherchali, M.E.H., Moulla, A.S., Amrous, K., Ouarezki, S.A., Rezka, A., Daas, N., 2021. The Continental Intercalaire Groundwaters of the Tidikelt (In-Salah Region, Algeria). Hydrochemical and Isotopic Features.

Clark, I., Fritz, P., 1997. Environmental Isotopes in Hydrogeology. Lewis Publishers, New York.

Coplen, T.B., Wildman, J.D., Chen, J., 1991. Improvements in the gaseous hydrogen-water equilibration technique for hydrogen isotopes ratio analysis. Anal. Chem. 63, 910–912. https://doi.org/10.1021/ac00009a014.

Coplen, T.B., et al., 2002. Isotope-Abundance Variations of Selected Elements (IUPAC Technical Report). https://doi.org/10.1515/ci.2003.25.2.22.

Cook, P., Herczeg, A.L., 2001. Environmental Tracers in Subsurface Hydrology. Kluver Academic publishers.

Cornet, A. (Mission 1956-1957) : Mission Hydrogéologique Ahaggar - Tassili.

Darling, W.G., Sorensen, J.P.R., Newell, A.J., Midgley, J., Benhamza, M., 2018. The Age and Origin of Groundwater in the Great Western Erg Sub-basin of the North-Western Sahara Aquifer System: Insights from Krechba,. https://doi.org/10.1016/j.apgeochem.2018.07.016. Central Algeria.

Durozoy, G., Juillet 1959. Les ressources en eaux des Tassili Oua-N'Ahaggar, (Département des Oasis, Territoires de l'OCRS), (mission hiver 1958-1959).

Edmunds, W.M., 1981. The hydrogeochemical characterization of groundwaters in the Sirte basin, using strontium and other elements. In: The Geology of Lybia. Academic, San Diego, California, pp. 703–714.

Edmunds, W.M., Guendouz, A.H., Mamou, A., Moulla, A.S., Shand, P., Zouari, K., 2003. Groundwater evolution in the Continental Intercalaire aquifer of Southern Algeria and Tunisia: trace element and isotopic indicators. Appl. Geochem. 18, 805–822. https://doi.org/10.1016/s0883-2927(02)00189-0.

Fabre, J., 2005. Géologie du Sahara Central et Occidental. Tervuren African Geosciences Collection. MRAC, Tervuren, Belgique, p. 572p.

Ferguson, G., Cuthbert, M.O., Befus, K., Gleeson, T., McIntosh, Jennifer C., 2020. Nature Geoscience, vol. 13, pp. 592–594. September 2020. www.nature.com/naturegeoscience.

Fontes, J.-C., Garnier, J.-M., 1979. Determination of the initial 14C activity of total dissolved inorganic carbon, A review of existing models and a new approach. Water Resour. Res. 15, 389–413.

Fontes, J.-Ch, Yousfi, M., Allison, G.B., 1986. Estimation of long term, diffuse groundwater discharge in the northern Sahara using stable isotope profiles in soil water. J. Hydrol. 86, 315–327.

Fritz, P., Fontes, J.Ch, 1980. Handbook of Environmental Isotopes Geochemistry, ume 1. The Terrestrial Environment,A. Elsevier Scientific Publishing Company.

Genet, Ed, Guyot, J., 1955. Etude chimique des eaux des régions Ahaggar - Tassili.

Gonfiantini, R., Conrad, G., Fontes, J-Ch, Sauzay, G., Payne, B.R., 1974. Etude isotopique de la nappe du Continental Intercalaire et ses relations avec les autres nappes du Sahara septentrional (Isotopic investigation of the Continental Intercalaire aquifer and its relationship with the other aquifers in the northern Sahara). In: Isotope Techniques in Groundwater Hydrology, vol. 1, pp. 227–241. IAEA SM-182/25, Vienna.

Guendouz, A., 1985. Contribution à l'étude géochimique et isotopique des nappes profondes du Sahara Nord-Est Septentrional, Algérie. Thèse de 3ème cycle, Université de Paris Sud. Centre d'Orsay.

Guendouz, A., Moulla, A.S., Edmunds, W.M., Shand, P., Poole, J., Zouari, K., Mamou, A., 1998. Palaeoclimatic information contained in groundwaters of the Grand Erg Oriental, North Africa. Isotope techniques in the study of past and current environmental changes in the hydrosphere and the atmosphere. In: Proc. Symp. IAEA, pp. 555–571.

Guendouz, A., Moulla, A.S., Edmunds, W.M., Zouari, k, Shand, P., Mamou, A., 2003. Hydrogeochemical and isotopic evolution of water in the Complexe Terminal aquifer in the Algerian Sahara. Hydrogeol. J. 11, 483–495. https://doi.org/10.1007/s10040-003-0263-7.

I.A.E.A, 2005. TecDoc 1453: Isotopic Composition of Precipitation in the Mediterranean Basin in Relation to Air Circulation Patterns and Climate.

IAEA/WMO, 2006. Global Network of Isotopes in Precipitation. The GNIP Database. http://isohis.iaea.org.

IAEA, 2008. Environmental Isotopes in the Hydrological Cycle. Principles and Applications, ume 1. Introduction: Theory, Methods, Review. Vienna.

Idrotecneco-Sonarem, 1975. Étude de la modélisation et évaluation des ressources en eaux de l'Ahaggar, et modélisation du synclinal de Tin-Séririne.

Jasechko, et al., 2015. Late-glacial to late-Holocene shifts in global precipitation $\delta^{18}O$. Clim. Past 11, 1375–1393. https://doi.org/10.5194/cp-11-1375-2015, 2015.

Kendall, C., McDonnell, J.J., 1998. Isotopes Tracers in Catchment Hydrology. Elsevier. https://doi.org/10.1016/c2009-0-10239-8.

Kinga, R., Coplen, T.B., 2008. Determination of the δ ($^2H/^1H$) of water: RSIL lab code 1574, chap. C1 of. In: Kinga-Révész, Coplen, T.B. (Eds.), Methods of the Reston Stable Isotope Laboratory. U.S. Geological Survey Techniques and Methods 10–C1, p. 27. https://doi.org/10.3133/tm10c1.

L'Annunziata, M.F., 2003. Handbook of Radioactivity Analysis. Academic Press (Handbook of Radioactivity Analysis).

Liégeois, J.P., Latouche, L., Boughrara, M., Navez, J., Guiraud, M., 2003. The LATEA metacraton (Central Hoggar, Tuareg shield, Algeria): behaviour of an old passive margin during the Pan-African orogeny. J. Architect. Educ. 37 https://doi.org/10.1016/j.jafrearsci.2003.05.004, 2003.

Liégeois, J.P., Benhallou, A., Azzouni-Sekkal, A., Yahiaoui, R., Bonin, B., 2005. The Hoggar Swell and Volcanism: Reactivation of the Precambrian Tuareg Shield during Alpine Convergence and West African Cenozoic Volcanism. Geological Society of America. https://doi.org/10.1130/0-8137-2388-4.379.

Liégeois, J.-P., Abdelsalam, M.G., Ennih, N., Ouabadi, A., 2013. Metacraton: nature, genesis and behavior. Gondwana Res. 23, 220–237. https://doi.org/10.1016/j.gr.2012.02.016.

Liégeois, J.P., 2019. A New Synthetic Geological Map of the Tuareg Shield: an Overview of its Global Structure and Geological Evolution. Springer Geology, pp. 83–107. https://doi.org/10.1007/978-3-319-96794-3_2.

McCrea, J.M., 1950. On the isotope chemistry of carbonates and a paleotemperature scale. J. Chem. Phys. 18, 849–857. https://doi.org/10.1063/1.1747785.

Moulla, A.S., Guendouz, A., Cherchali, M.E.H., Chaid, Z., Ouarezki, S.A., 2012. Updated geochemical and isotopic data from the Continental Intercalaire aquifer in the Great Occidental Erg sub-basin (south-western Algeria). Quat. Int. 257, 64–73. https://doi.org/10.1016/j.quaint.2011.08.038, 2012.

Négrel, P., Petelet-Giraud, E., Vidory, D., 2004. Strontium isotope geochemistry of alluvial groundwater: a tracer for groundwater resources characterization. Hydrol. Earth Syst. Sci. 8 (5), 959–972. https://doi.org/10.5194/hess-8-959-2004, 2004.

Négrel, P., Casanova, J., 2005. Comparison of the Sr isotopic signatures in brines of the Canadian and Fennoscandian shields. Appl. Geochem. 20, 749–766. https://doi.org/10.1016/j.apgeochem.2004.11.010, 2005.

Négrel, P., 2006. Water-granite interaction: clues from strontium, neodymium and rare earth elements in soil and waters. Appl. Geochem. 21, 1432–1454. https://doi.org/10.1016/j.apgeochem.2006.04.007, 2006.

Pearson, F.J., Hanshaw, B.B., 1970. Isotope Hydrology 1970. In: Source of Dissolved Carbonate Species in Groundwater and Their Effects on Carbon-14 Dating. IAEA, Vienna, pp. 271–276.

Reardon, E.J., Fritz, P., 1978. Computer modelling of groundwater 13C and 14C isotope compositions. J. Hydrol. 36, 210–224.

Rougier, et al., 2013. Eocene exhumation of the Tuareg shield (Sahara desert, Africa). Geology 41 (5), 615–618. https://doi.org/10.1130/g33731.1. May 2013.

Saighi, O., 1999. Hydrogéologie en zones arides. Hydrochimie isotopique des eaux naturelles de l'Ahaggar et modélisation de la nappe d'inféro-flux. Université des Sciences et de la Technologie Houari Boumédienne, Alger.

Saighi, O., Michelot, J.L., Filly, A., 2001. Isotopic Characteristics of Meteoric Water and Groundwater in Ahaggar Massif (Central Sahara).

Saighi, O., 2005. Isotopic Composition of Precipitation from Algiers and Assekrem in IAEA-TecDoc-1453: Isotopic Composition of Precipitation in the Mediterranean Basin in Relation to Air Circulation Patterns and Climate Final Report of a Coordinated Research Project 2000–2004 October 2005.

Schofield, S., Jankowski, J., 2004. Hydrochemistry and Isotopic Composition of Na–HCO_3-Rich Groundwaters from the Ballimore Region. https://doi.org/10.1016/j.chemgeo.2004.06.026 central New South Wales, Australia.

Simler, R., 2020. Hydrochemistry Multilanguage Software Diagrammes Free Distribution Laboratory of Hydrogeology. University of Avignon, France. Version 6.7.

Skonieczny, C., Paillou, P., Bory, A., Bayon, G., Biscara, L., Crosta, X., Eynaud, F., Malaizé, B., Revel, M., Aleman, N., Barusseau, J.-P., Vernet, R., Lopez, S., Grousset, F., 2015. African humid periods triggered the reactivation of a large river system in Western Sahara. www.nature.com/naturecommunications.

Stumm, W; Morgan, J.J.: Aquatic Chemistry: Chemical Equilibria and Rates in Natural Waters. third ed..

Taylor, A.S., Blum, J.D., Lasaga, A.C., MacInnis, 2000. Kinetics of dissolution and Sr release during biotite and phlogopite weathering. Geochem. Cosmochim. Acta 64, 1191–1208.

White, W.M., 2005. Geochemistry.